EW Physics at LHC

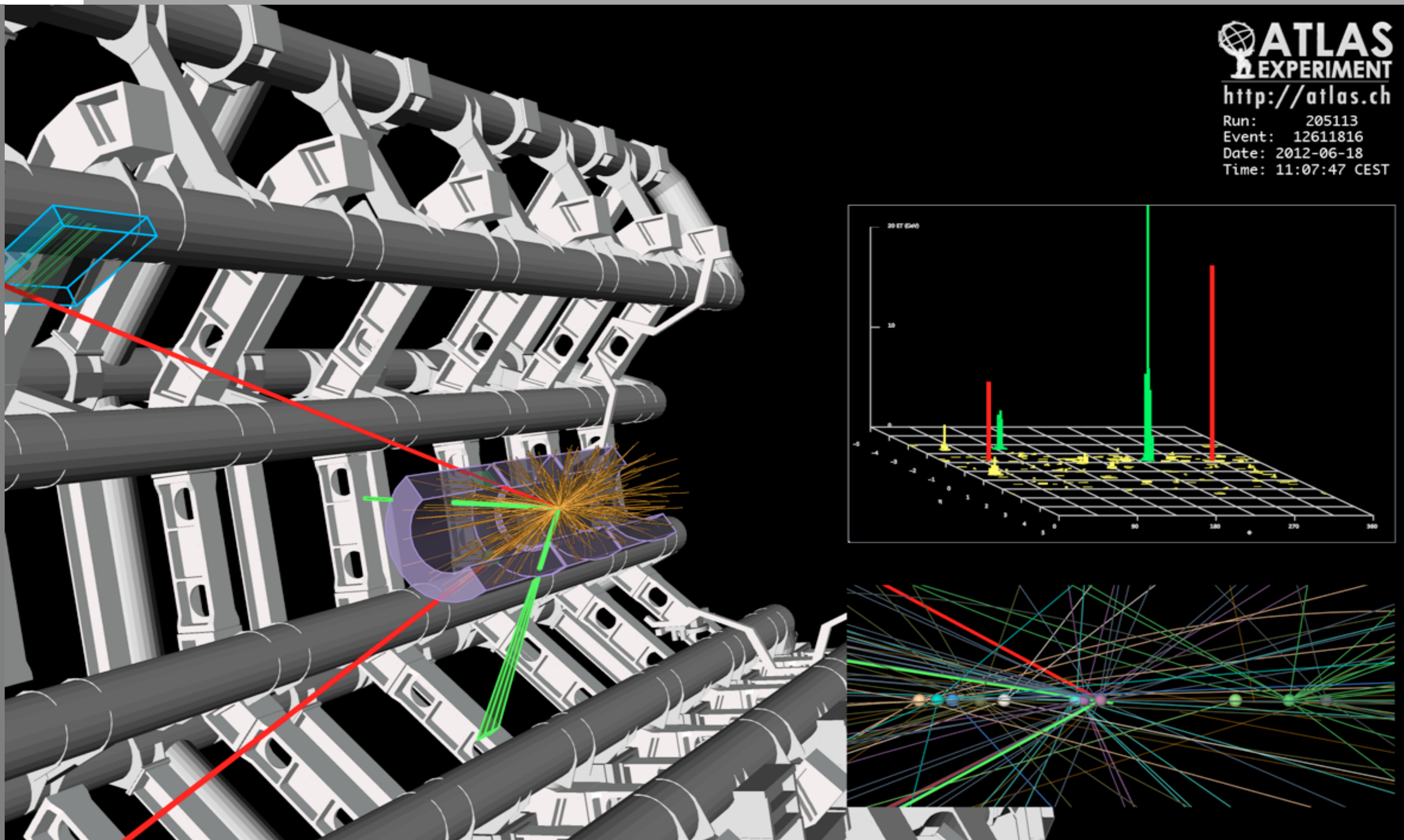

Event display of a 2e2mu candidate. EventNumber: 12611816 RunNumber: 205113 m_4l=123.9 GeV. m_12=87.9 GeV, m_34=19.6 GeV. e_1: pt=18.7 GeV, eta=-2.45, phi=1.68,. e_2: pt=75.96 GeV, eta=-1.16, phi=-2.13. mu_3: pt=19.6 GeV, eta=-1.14, phi=-0.87. mu_4: pt=7.9 GeV, eta=-1.13, phi=0.94

Contents

- Standard Candles
- W discovery & mass measurement
- W & Z cross sections. Ratios
- W mass measurement at LHC
- Di-bosons
- TGC & QTGC

Standard Candles

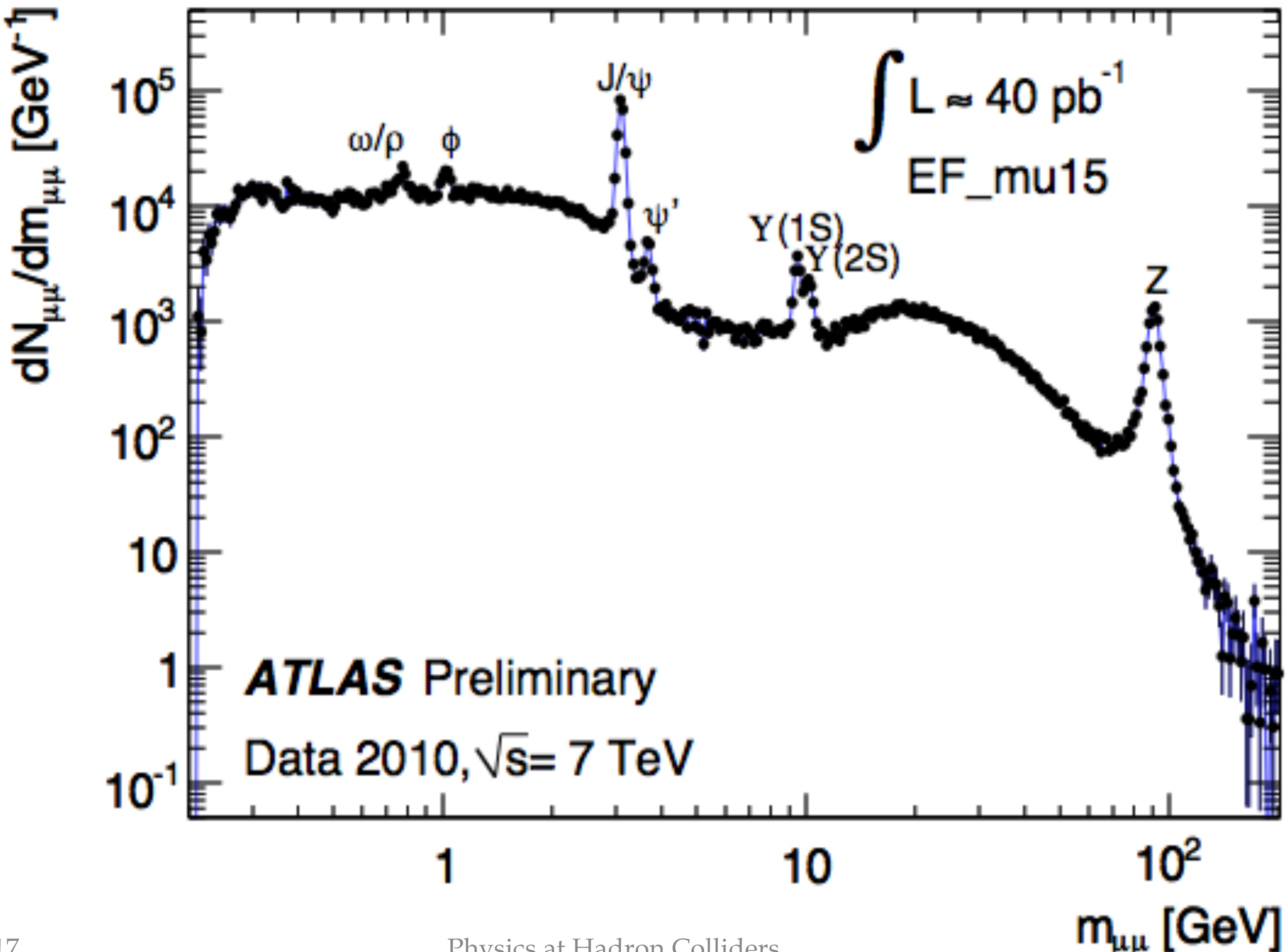

W/Z discovery at the SPS

Discovery at hadron collider: CERN SppS 1982/3

Proton-antiproton collider at 540 GeV [dominant production process: quark-antiquark annihilation]

Two multipurpose experiments: UA1, UA2

Signature: decay in leptons [clean, QCD background suppressed]

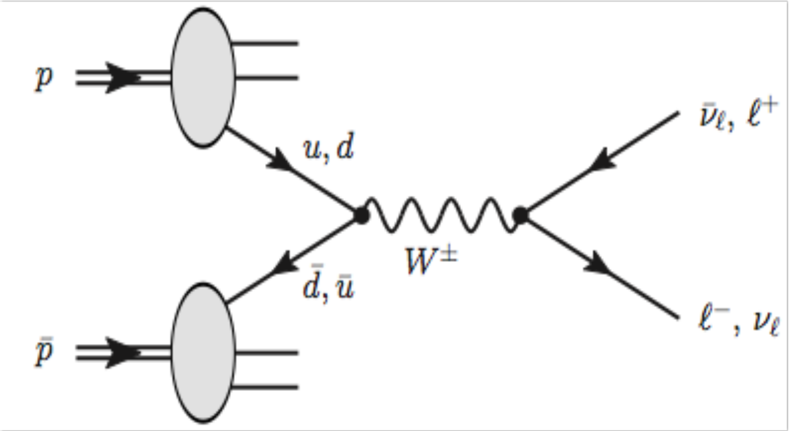

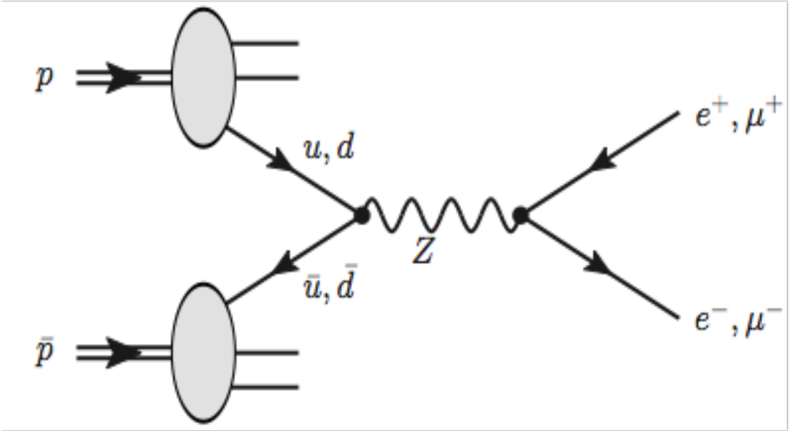

Z Candidates at UA2

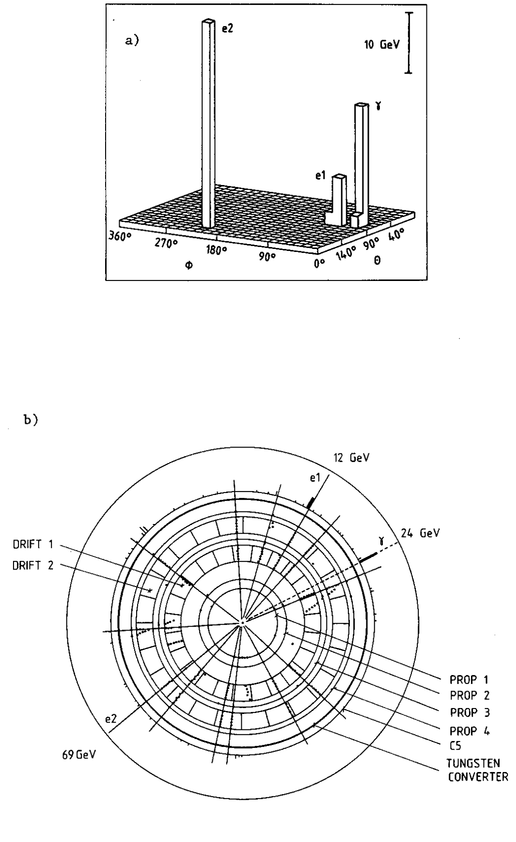

Figure 4

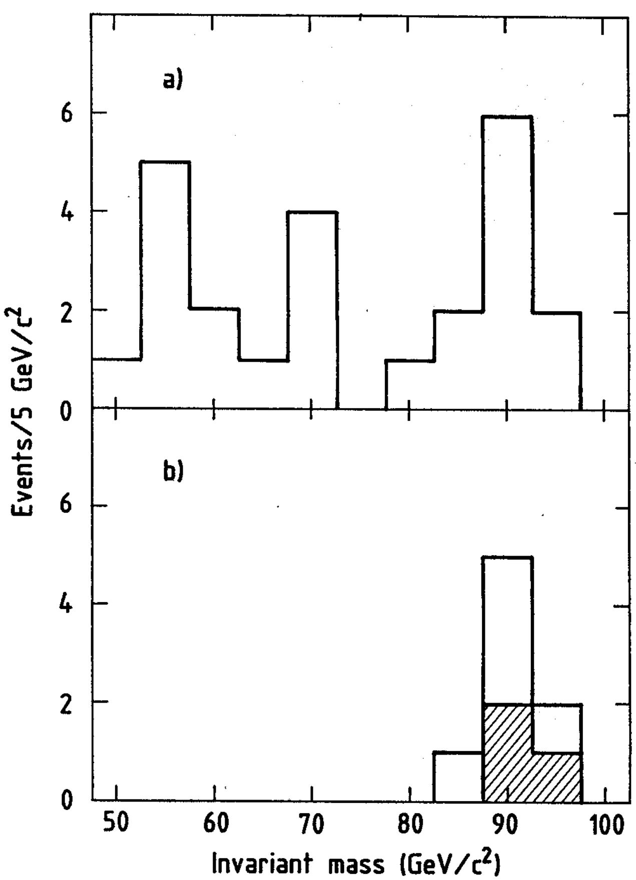

Invariant Mass of Electron Pairs
[P. Bagnia et al., Phys. Lett. B129 (1983) 130]

W & Z decays

Toni Baroncelli:

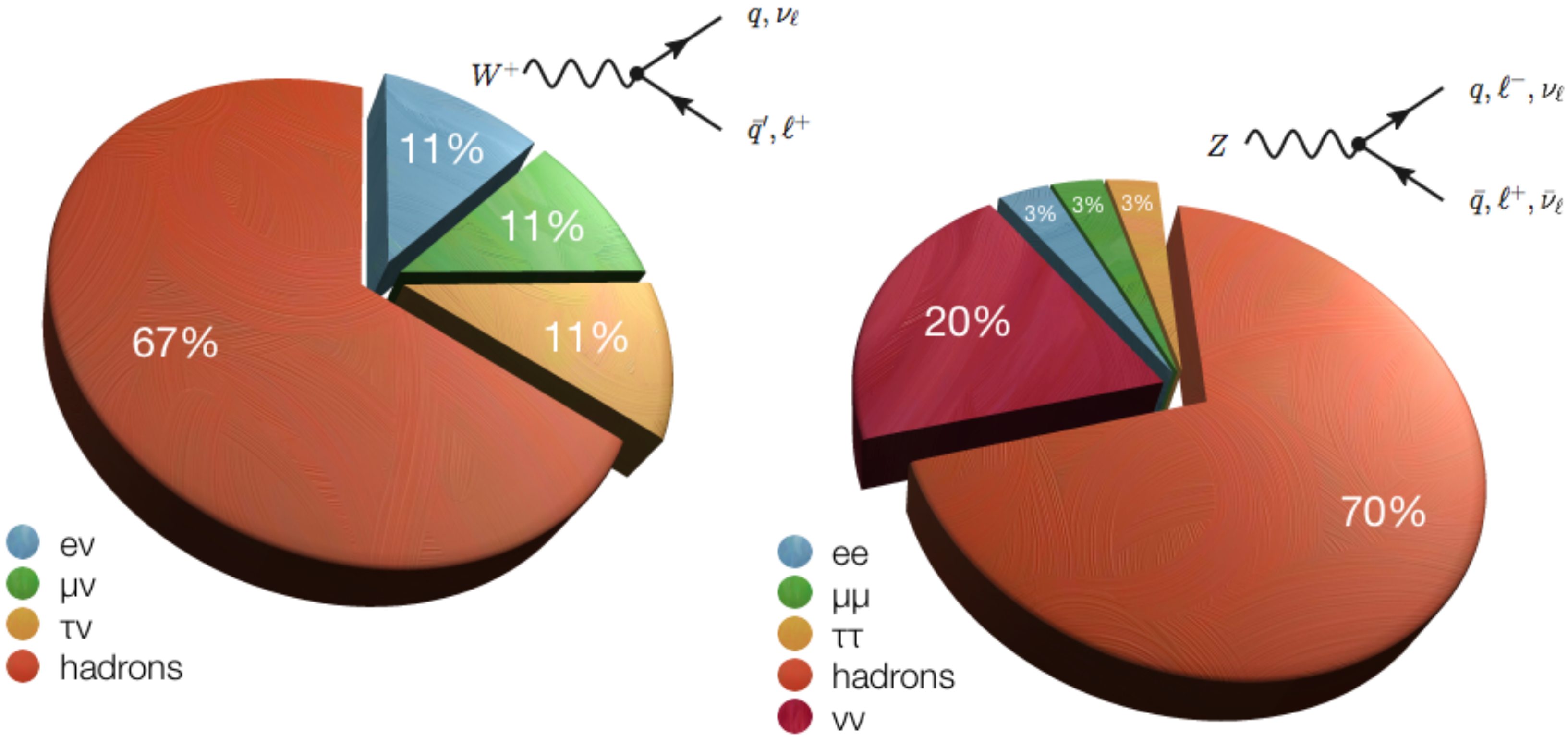

Leptonic decays (e/μ): very clean, but small(ish) branching fractions. Hadronic decays: two-jet final states; large QCD dijet background. Tau decays: somewhere in between…

Hadron Collider Signatures

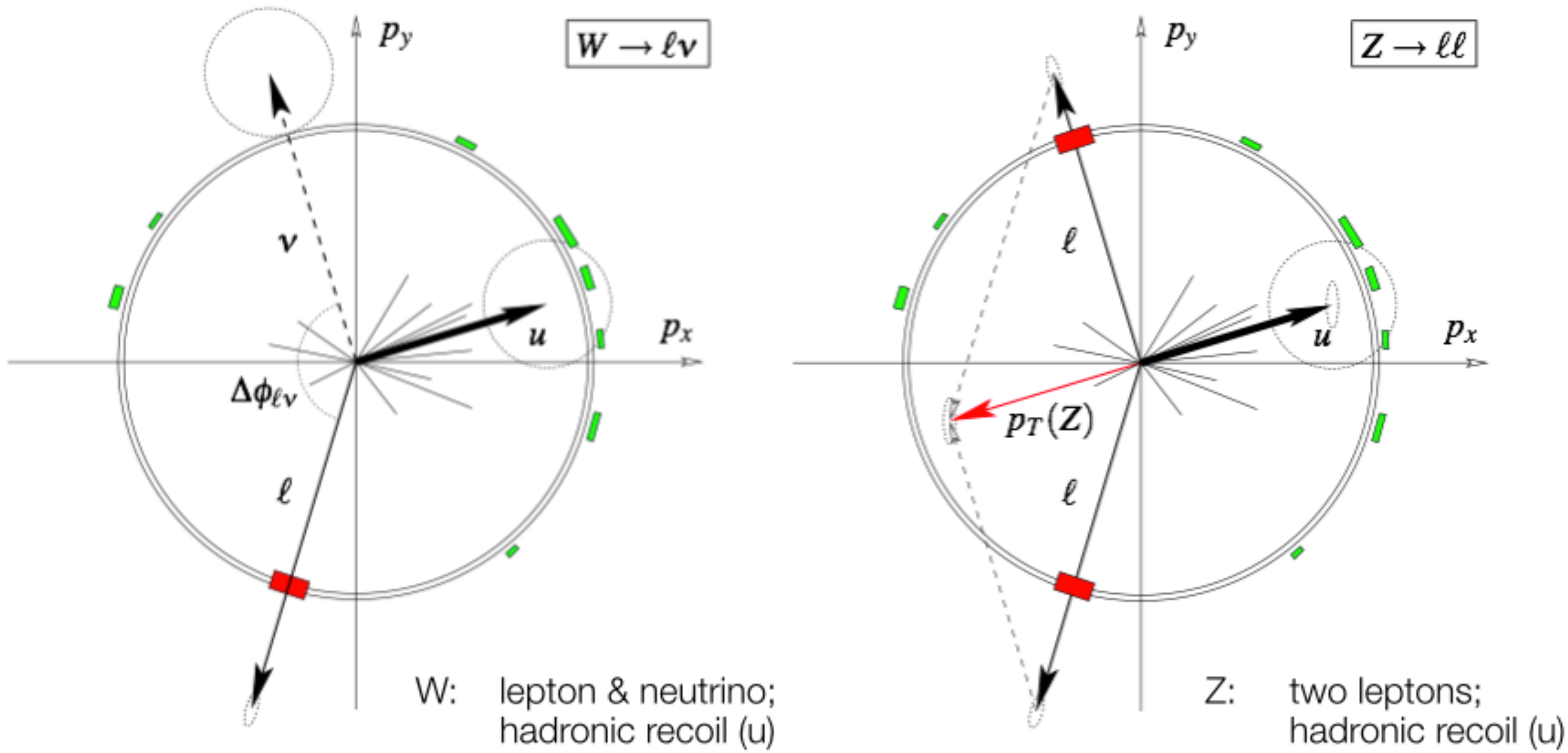

Additional hadronic activity ➛ recoil, not as clean as e^+e^-
Precision measurements: only leptonic decays

W/Z Production

Need quarks & anti-quarks!

Single W/Z production:

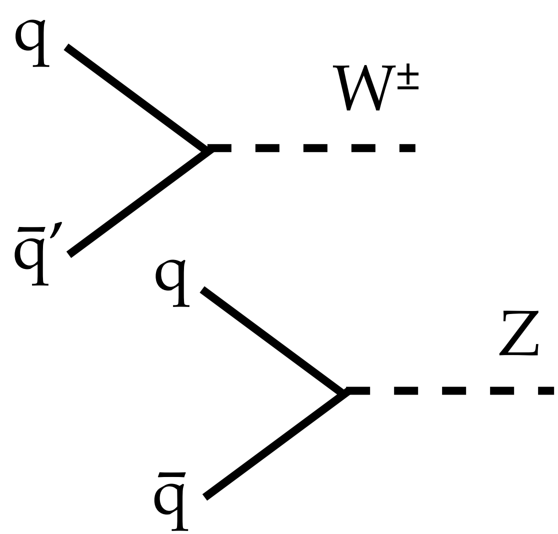

W production: (main contributions)

$$\begin{cases} u\bar{d} \to W^+ \\ d\bar{u} \to W^- \end{cases}$$

p = uud

Z production: (main contributions)

$$\begin{cases} u\bar{u} \to Z \\ d\bar{d} \to Z \end{cases}$$

- At LHC energies these processes take place at low values of Bjorken-x
- Only sea quarks are involved
- At EW scales sea is driven by the gluon i.e. x-sections dominated by gluon uncertainty

Comparison w/ Tevatron:

- pp-collider, i.e. valence anti-quarks available …
- W/Z production at higher x …

➡ Constraints on sea and gluon distributions

Z & W cross sections vs √s

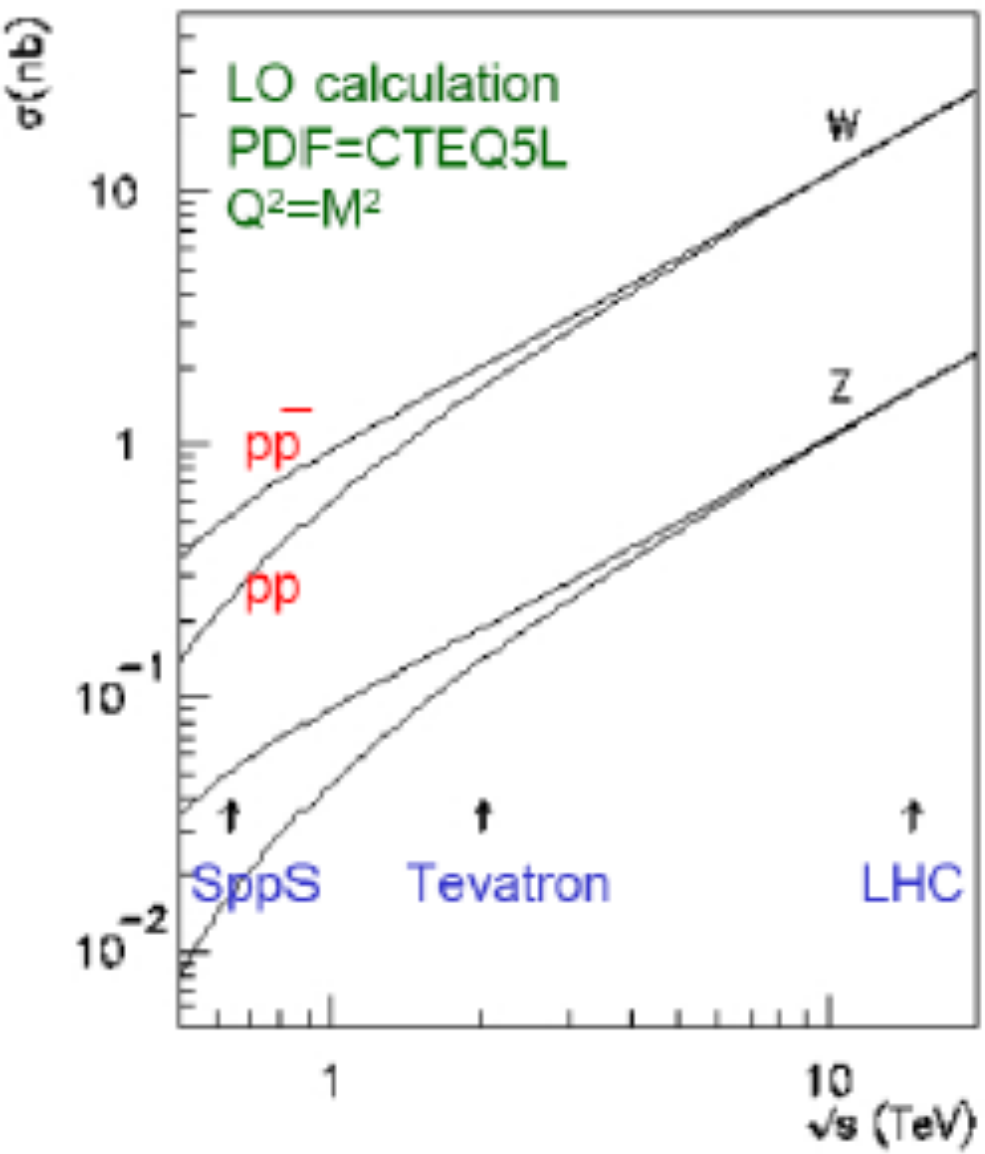

Differential Cross Section

NNLO cross sections:
scale uncertainties very small

W rapidity: asymmetry
[sensitivity to PDFs]

$$A_W(y) = \frac{d\sigma(W^+)/dy - d\sigma(W^-)/dy}{d\sigma(W^+)/dy + d\sigma(W^-)/dy}$$

Proton-Proton Collider:

symmetry around y=0 …

PDFs: u(x) > d(x) for large x …
more W^+ at positive rapidity

d/u ratio < 1 …
always more W^+ than W^-

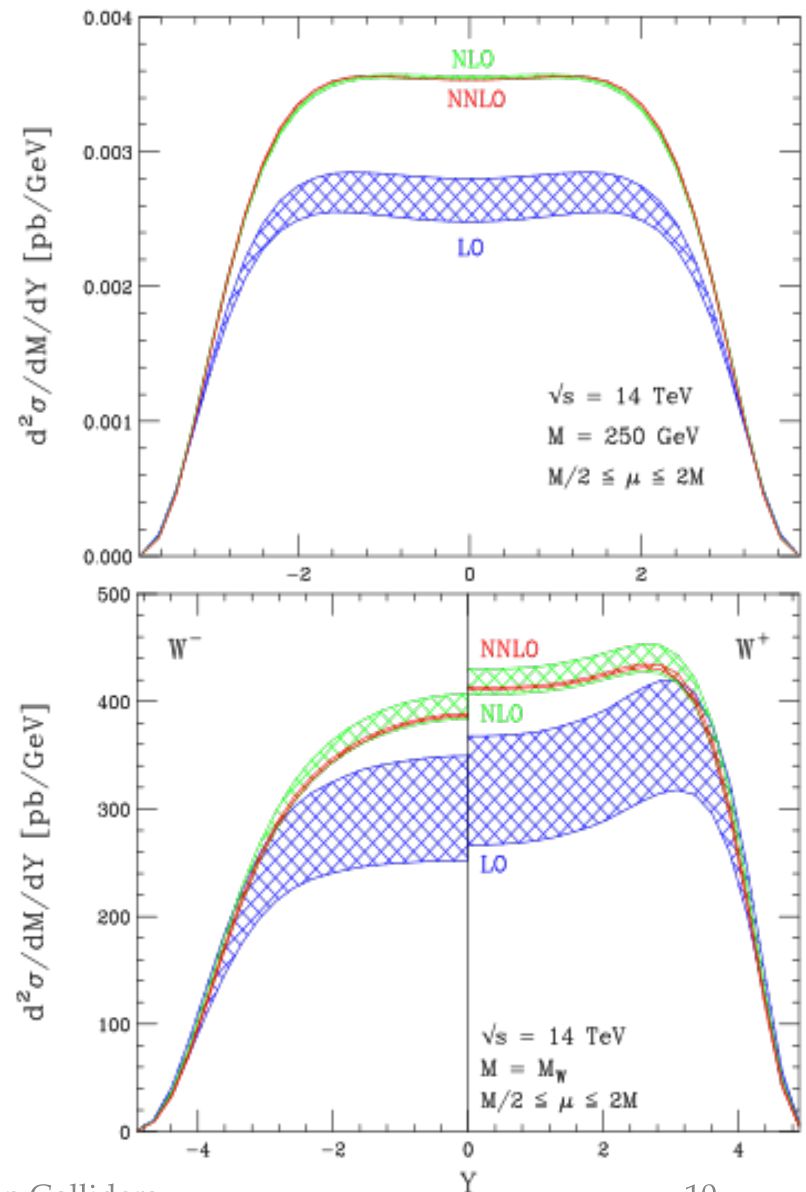

[C. Anastasiou et al., PRD 69 (2004) 094008]

Toni Baroncelli:

W^+/W^--Cross Section Ratio ...

W^+/W^- rapidity distributions

Define:

$$R_{\mp} = \frac{\sigma_{W^-}}{\sigma_{W^+}}$$

W production: (main contributions) $\left\{ \begin{array}{l} u\bar{d} \to W^+ \\ d\bar{u} \to W^- \end{array} \right.$

$$R_{\mp} \approx \frac{d\bar{u}}{u\bar{d}} \approx \frac{d}{u}$$

[assuming $\bar{d}/\bar{u}$ =1]

Differential

:

$$R_{\mp}(y_W) = \frac{d\sigma/dy_W(W^-)}{d\sigma/dy_W(W^-)}$$

$$\approx \frac{d(x_1)\bar{u}(x_2)}{u(x_1)\bar{d}(x_2)} \approx \frac{d(x_1)}{u(x_1)}$$

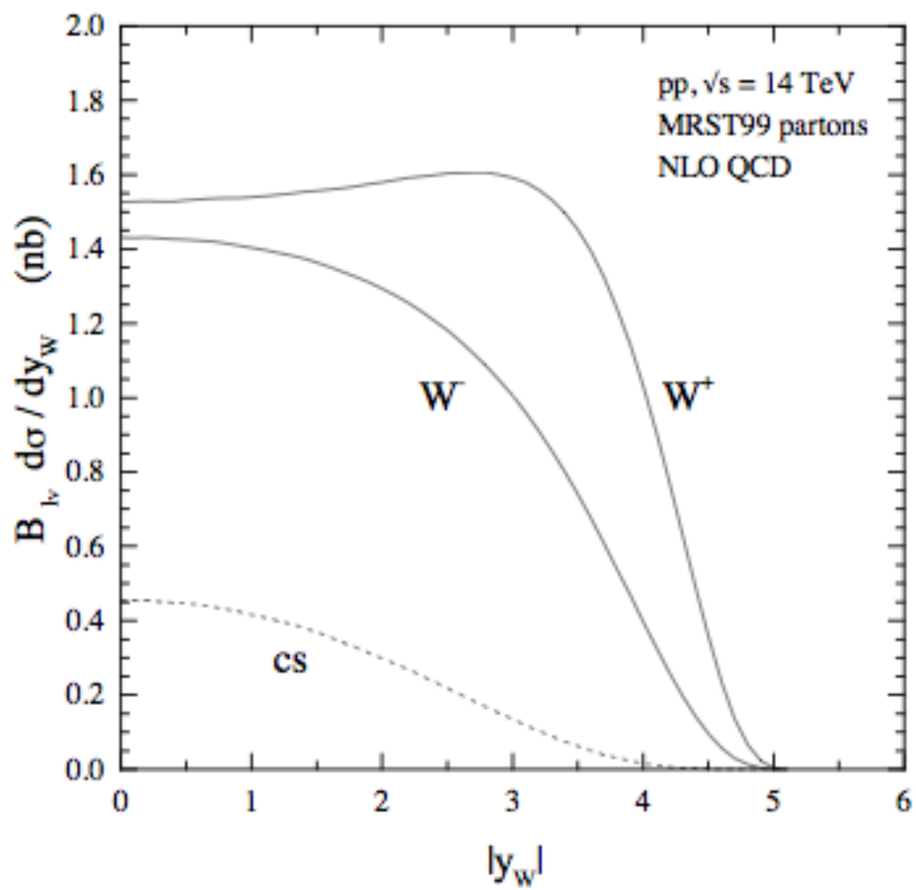

PDF Uncertainty on W-Production …

Toni Baroncelli:

$W^{\pm}$ rapidity distribution

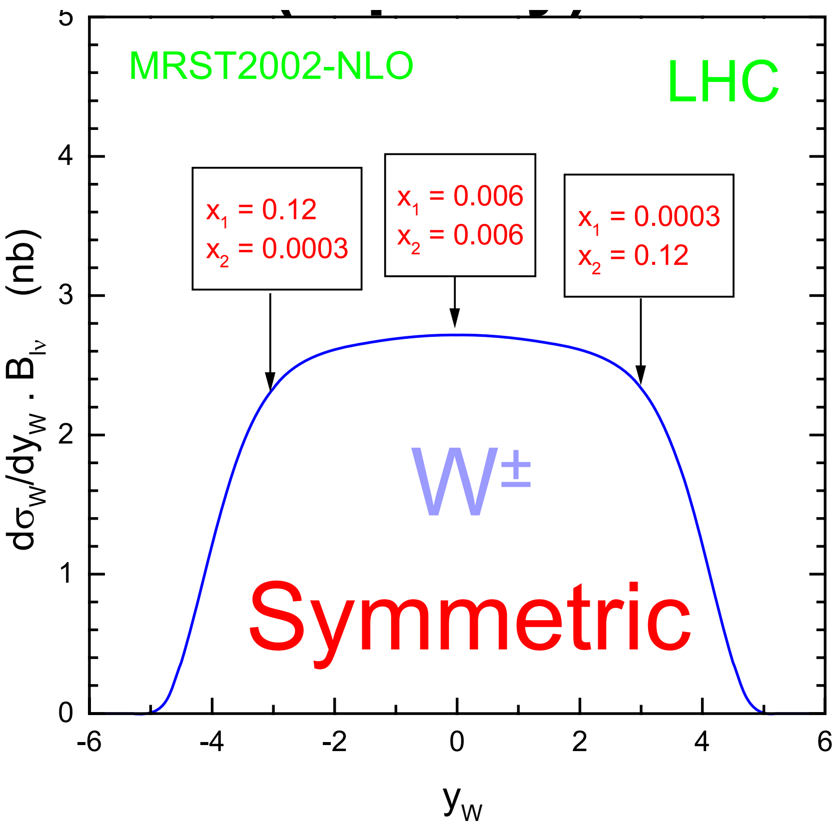

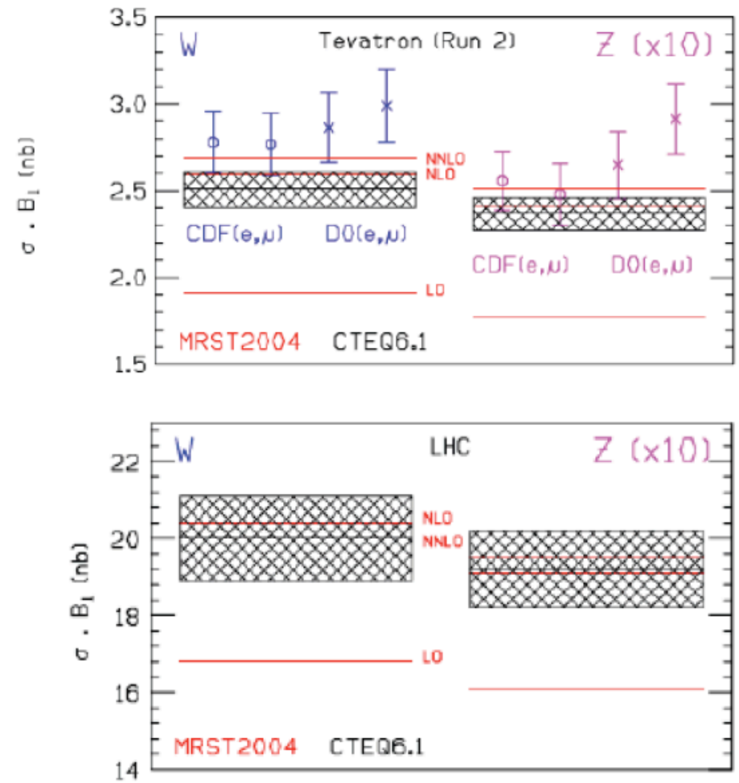

$W^{\pm}$ total cross section

4% MRST02 uncertainty

Theoretical uncertainty dominated by PDFs

Extra input from LHC measurements

Effect on PDFs of LHC W data

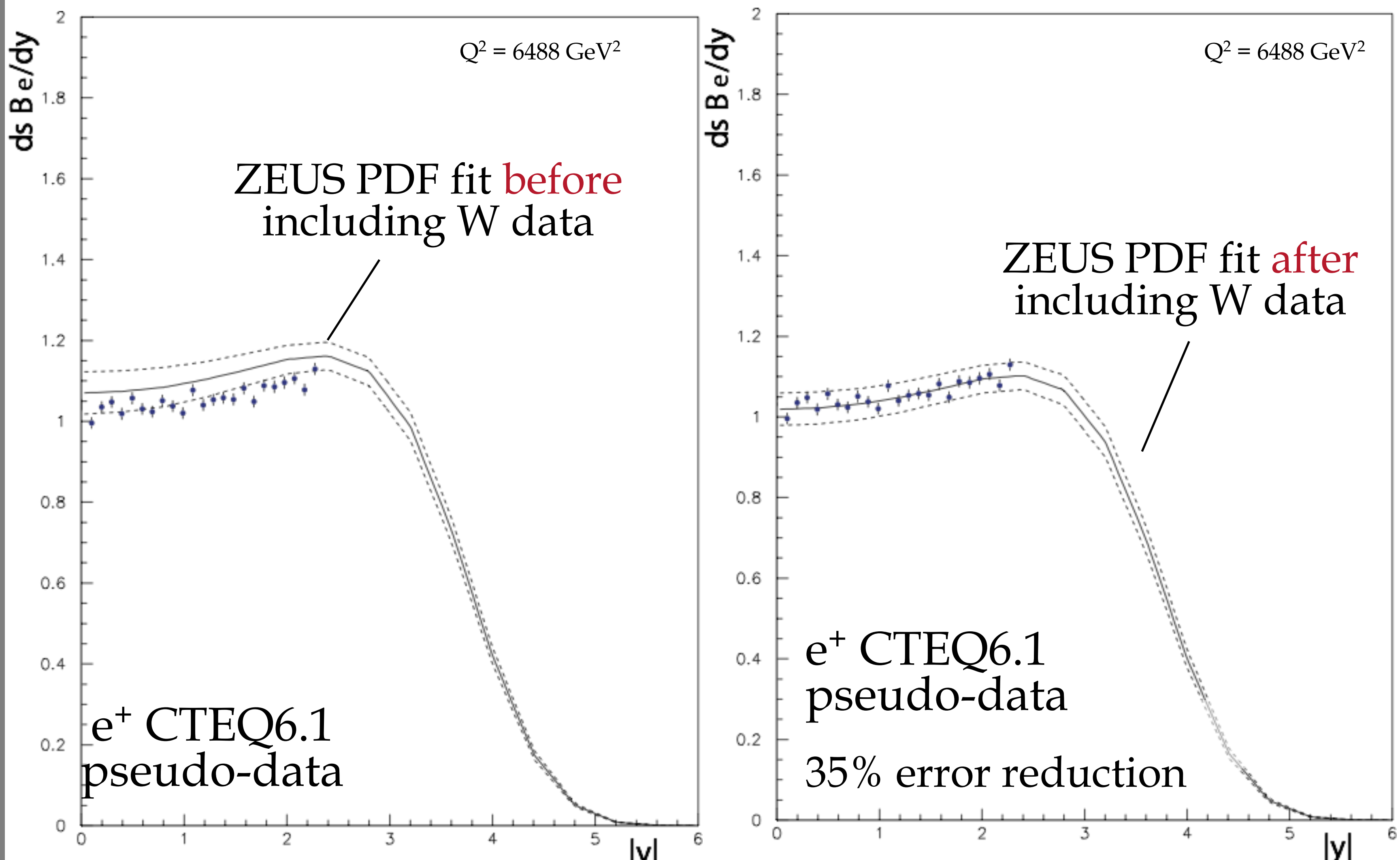

[Tricoli et al., arXiv:hep-ex/0509002v1]

W/Z at Tevatron

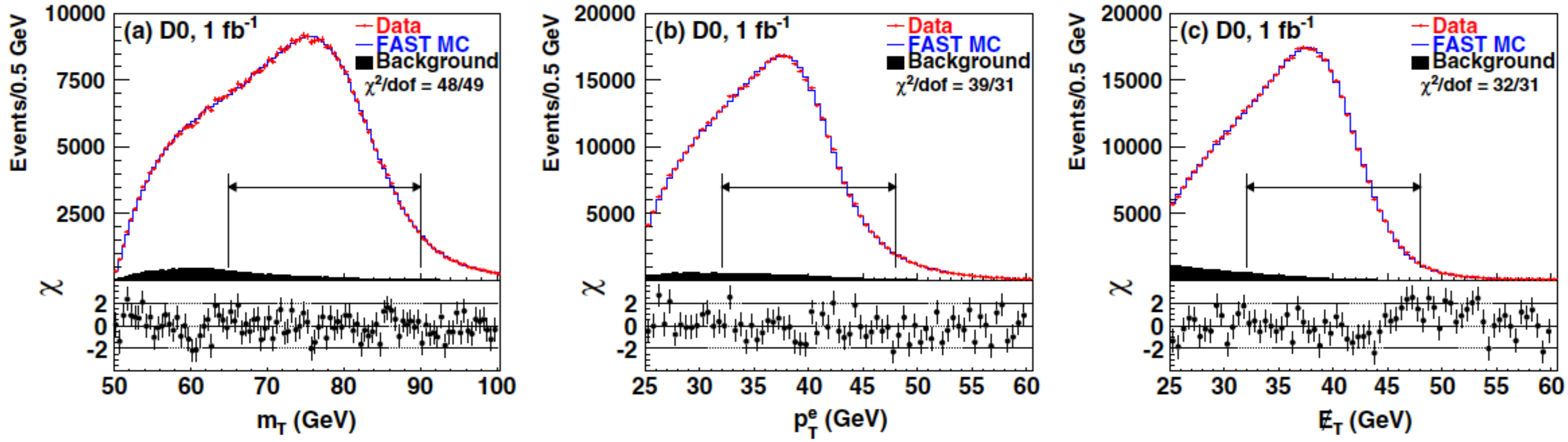

Tevatron: pp-collider [$\sqrt{s}$ = 1.8 TeV and 1.96 TeV]

W/Z cross sections;
asymmetries ...

Most precise W mass measurement to date ...

Diboson production, i.e. WW, WZ, ZZ ...

W/Z + jet production … [major background for top physics]

[V. M. Abazov et al., Phys. Rev. Lett. 103 (2009) 141801]

Isolated High-p_T Leptons

Starting point for many hadron collider analyses:
isolated high-p_T leptons ➛ discriminate against QCD jets ...

QCD jets can be mis-reconstructed as leptons ("fake leptons")

QCD jets may contain real leptons e.g. from semileptonic B decays [B ➛ lνX]

➛ soft and surrounded by other particles

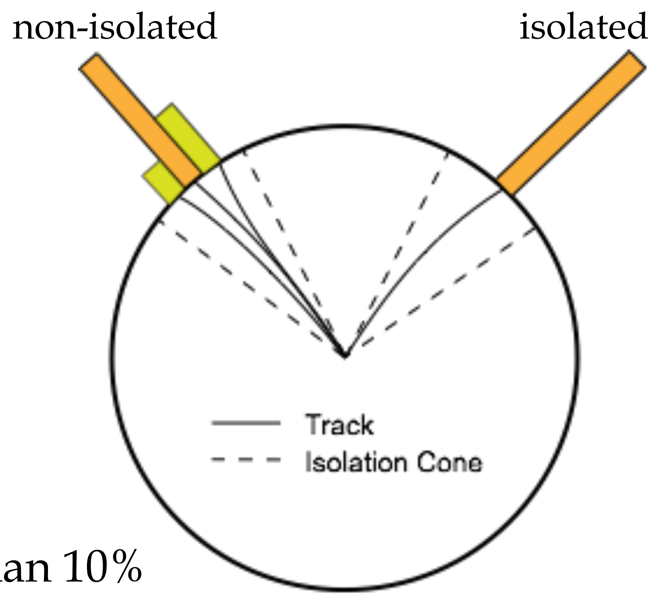

"Tight" lepton selection ...

Require e/μ with p_T > (at least) 20 GeV
Track isolation, e.g. $\sum p_T$ of other tracks in cone of ΔR=0.1 less than 10% of lepton p_T

Calorimeter isolation, e.g. energy deposition from other particles in cone of ΔR=0.2 less than 10%

$W^{\pm}$ Signal & Control Regions

Signal Region (SR) contains events we want to select, Control Regions are close to SR but ortogonal.

SR: Lepton quality & trigger match & E_T^{miss} > 25 GeV & m_T > 50 GeV & lepton isolation & Overlap Removal (OR)

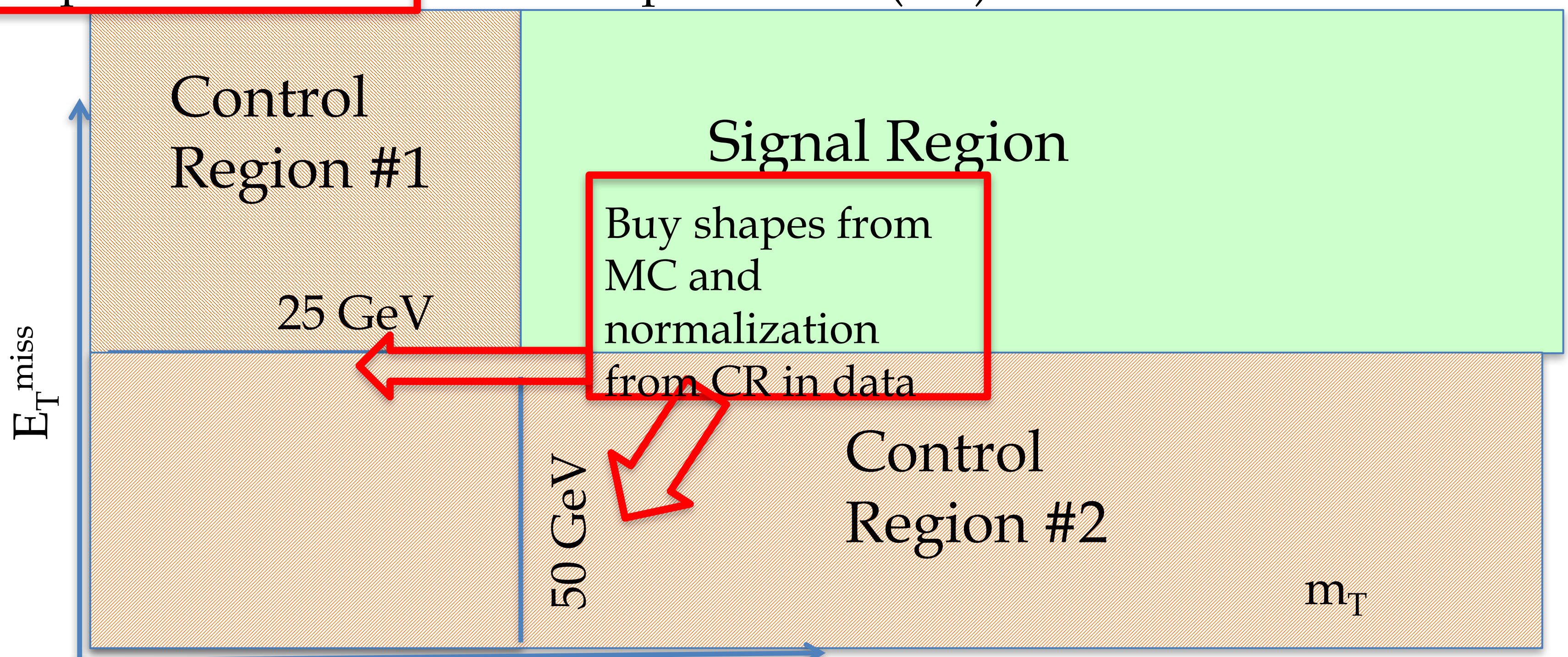

Background from heavy flavours decays and (for electrons) photon conversions determined using a “data-driven” technique.

Extrapolating from CR to SR

The number of multijet events versus the isolation variable for the $W \rightarrow e\nu$ (left) and $W \rightarrow \mu\nu$ (right) analysis is shown. The plots illustrate the multijet-evaluation methodology for the W^+ analysis. The results obtained for two of the four discriminant variables used to evaluate the multijet yields are shown for both types of isolation: m_T (circles) and p_T^ℓ (squares) with calorimeter-based isolation and m_T (triangles) and p_T^ℓ (stars) with track-based isolation. **Open markers represent the yields obtained with the E_T^{miss} fit region while closed markers are those with the m_T fit region.** The points represent the extracted multijet fraction from the fit of the variables, in the isolation intervals represented on the x-axis for the template selection. The lines represent the linear extrapolation of the points to the signal region. The definition of the signal region is p_T and isolation-flavour dependent but corresponds approximately to the region of isolation below 0.1 in these plots. The error bar in each bin represents the uncertainty from the fit of the variable rescaled by the square root of the reduced χ^2 of the fit.

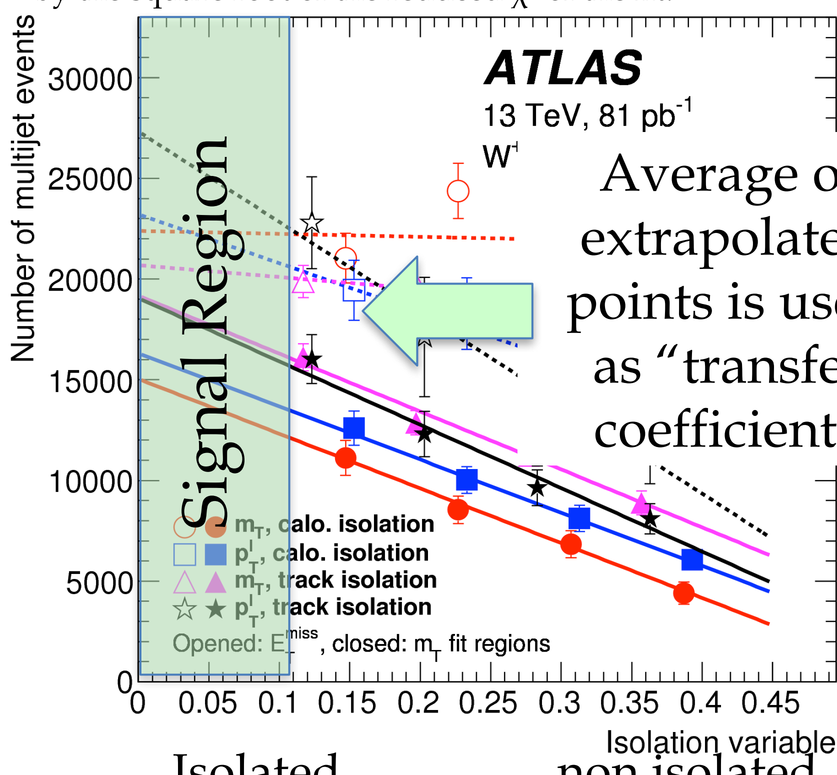

Average of extrapolated points is used as "transfer coefficient"

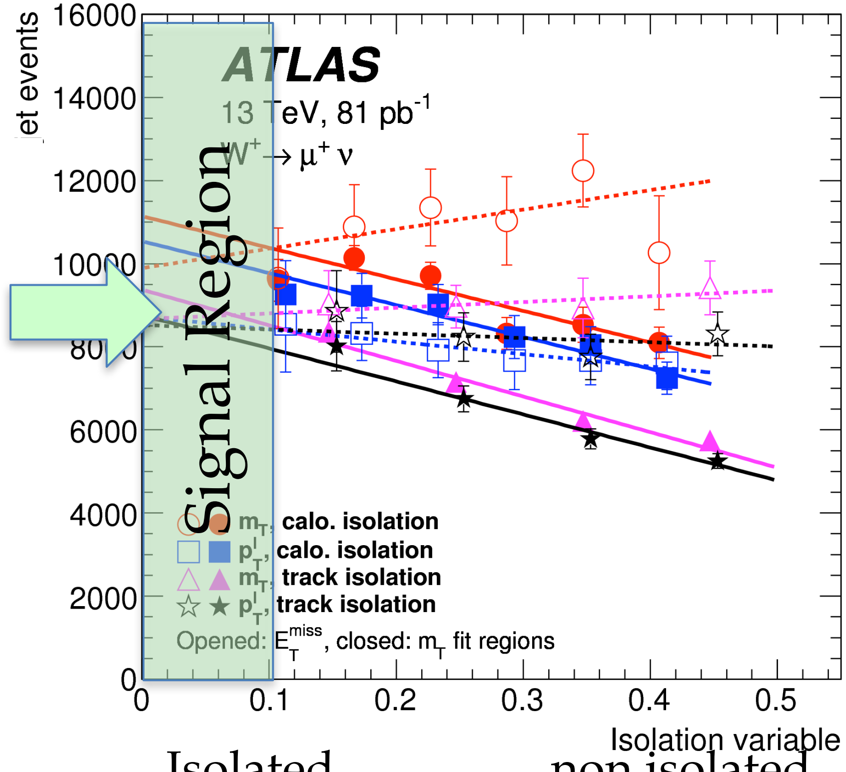

Transverse mass distributions from the W →lν

Measurement of W± and Z-boson production cross sections in pp collisions at √s = 13 TeV with the ATLAS detector, *Phys. Lett. B 759 (2016) 601*

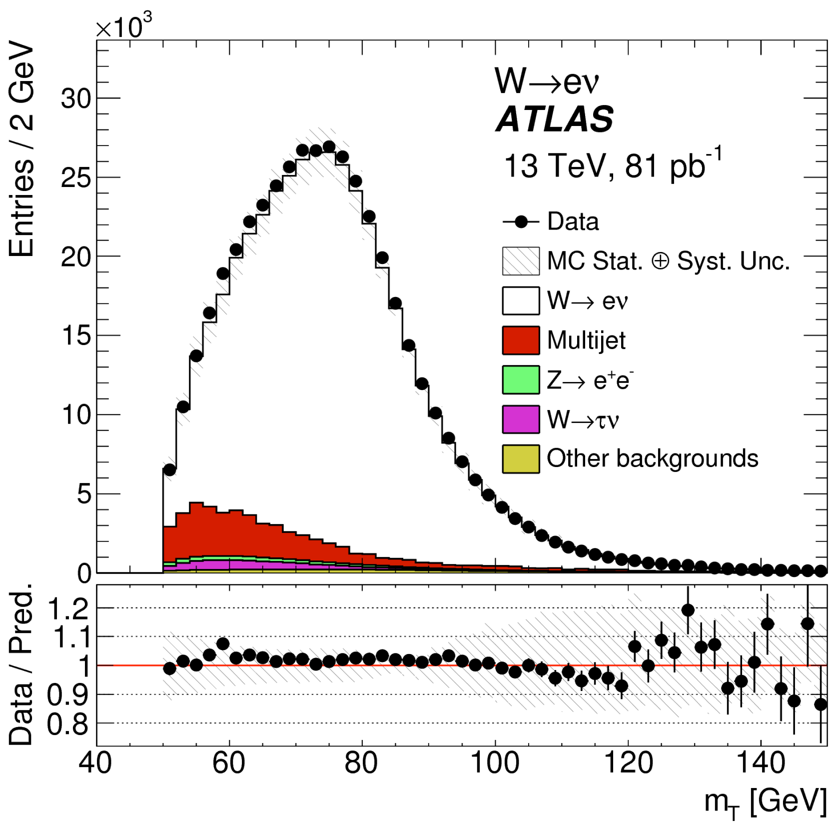

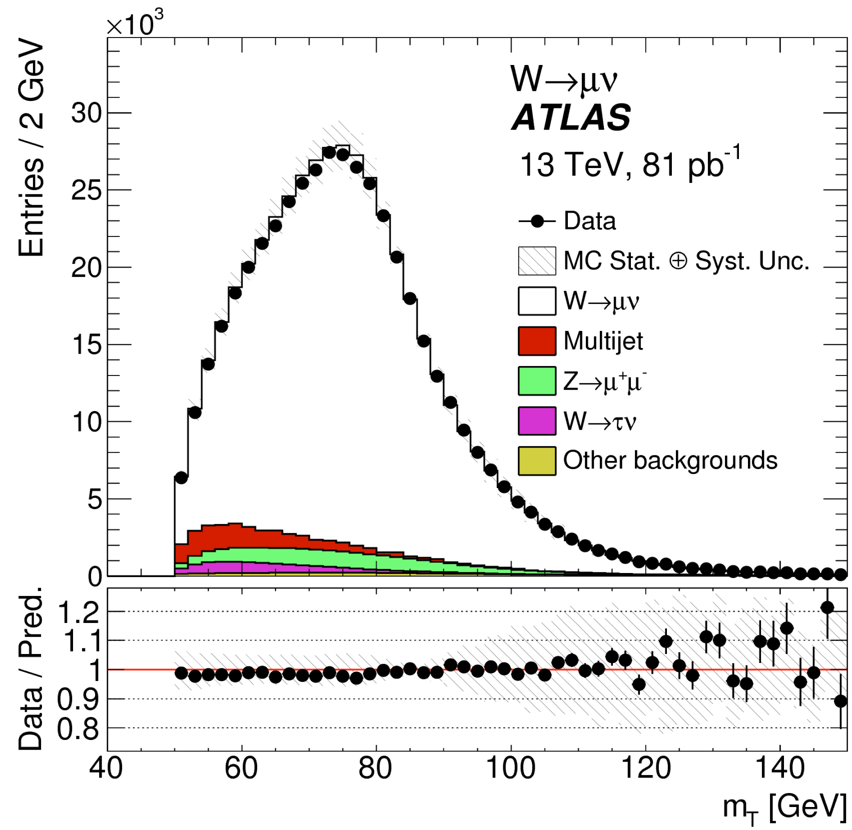

Toni Baroncelli:

dilepton mass distributions from the $Z \rightarrow ll$

Measurement of W± and Z-boson production cross sections in pp collisions at $\sqrt{s}$ = 13 TeV with the ATLAS detector, *Phys. Lett. B 759 (2016) 601*

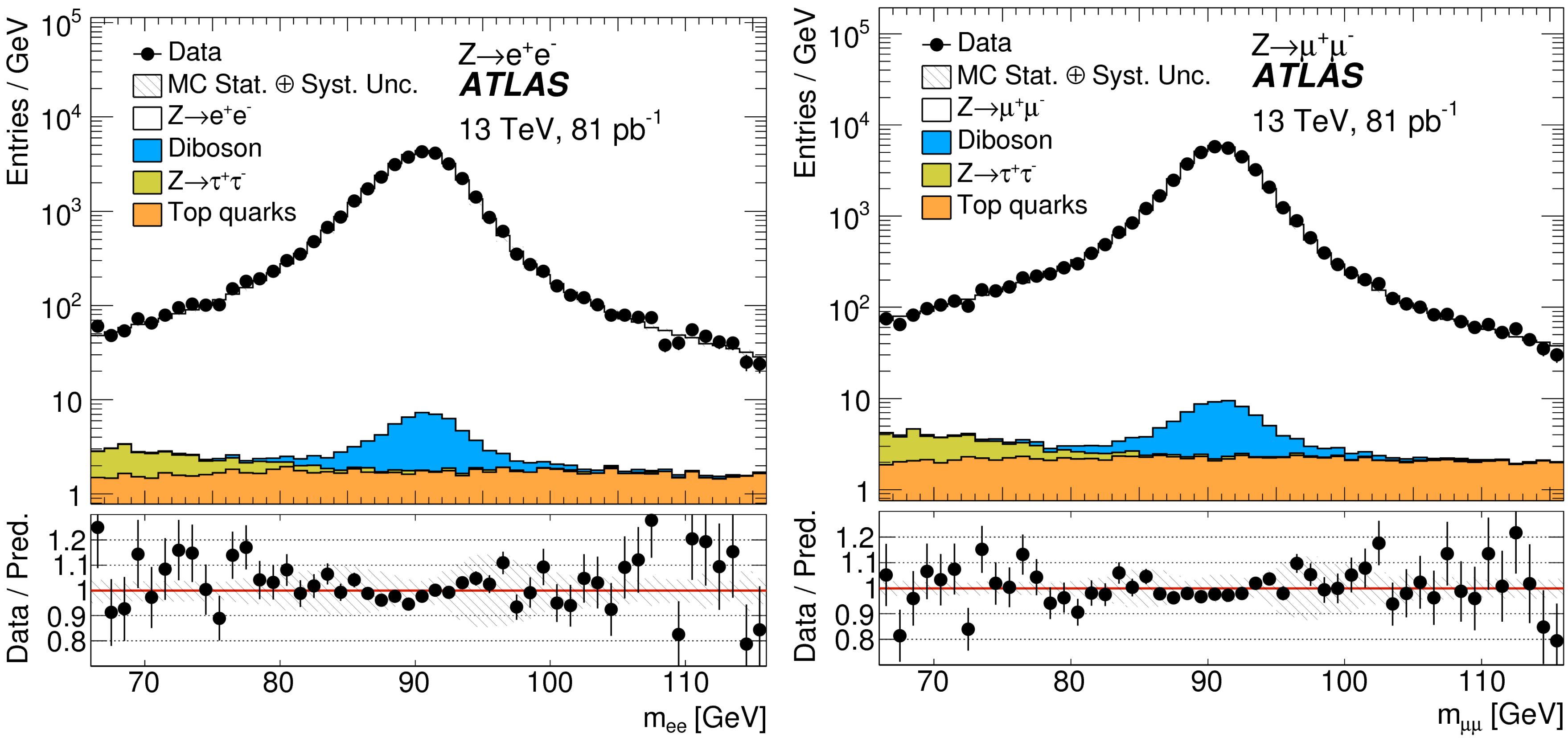

SR: Lepton quality & trigger match exactly two selected leptons of the same flavour but of opposite charge with invariant mass of

$66 < m_{ll} < 116$ GeV.

Ratio of Cross Sections

Ratio of the electron- and muon-channel W and Z-boson production fiducial cross sections, compared to the expected values of the Standard Model of (1,1) (neglecting mass effects that contribute at a level below 10^{-5}) and previous experimental verifications of lepton universality for on-shell W and Z bosons, shown as PDG average bands. The PDG average values and the result are shown with total uncertainties.

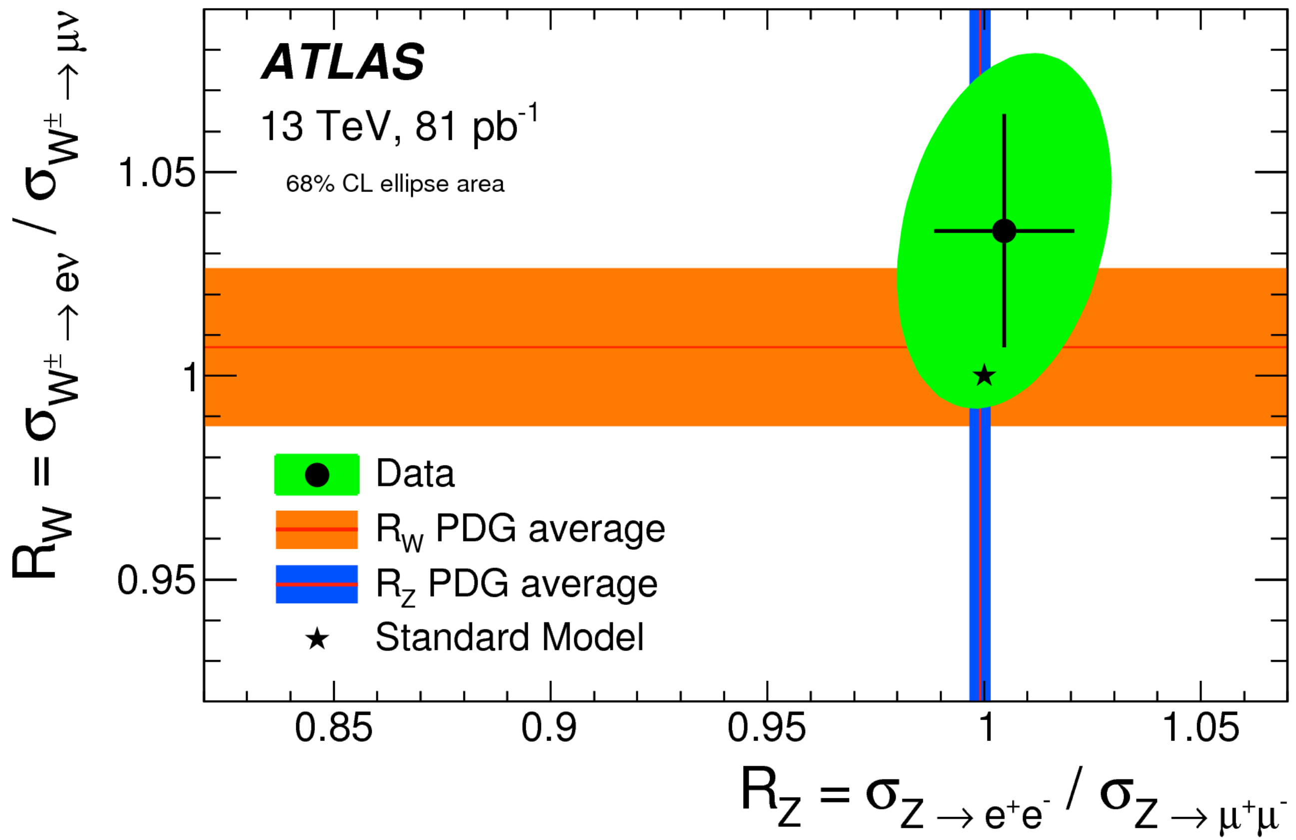

Results

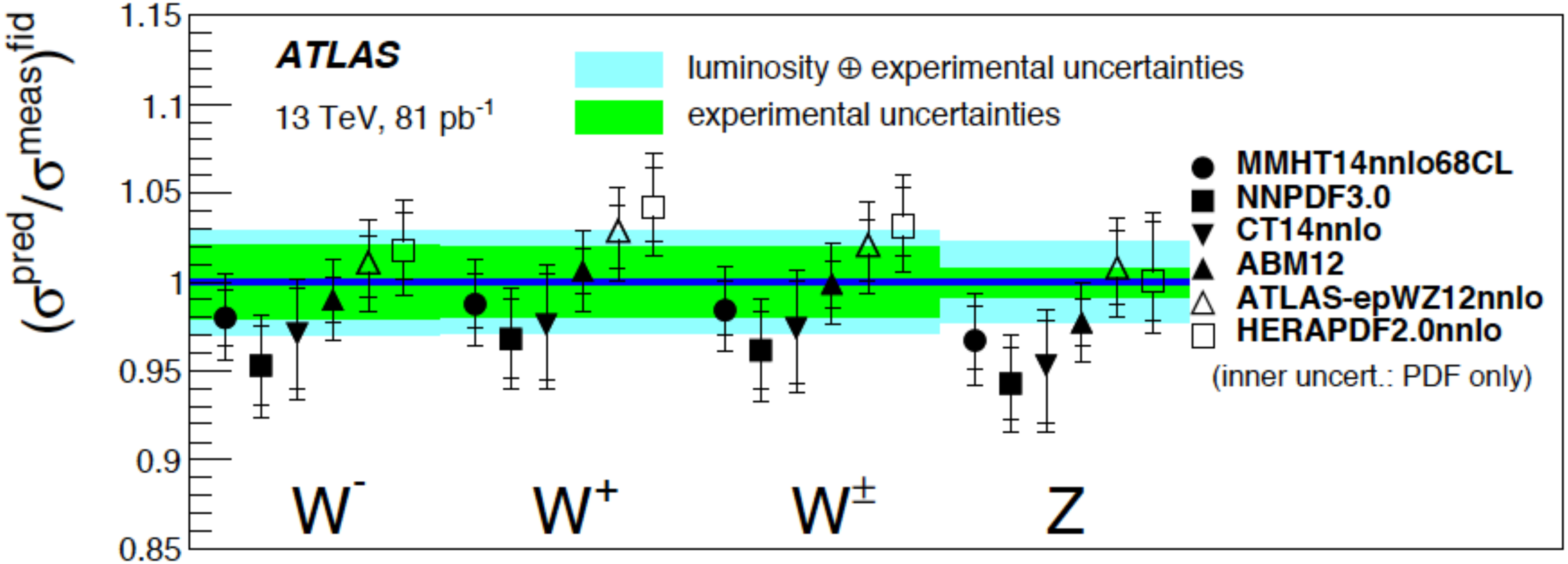

	W^+	W^-	Z
	Electron channel (value ± stat ± syst ± lumi)		
Signal events	228060 ± 510 ± 4920 ± 200	177890 ± 450 ± 6110 ± 180	34865 ± 187 ± 7 ± 3
Correction C	0.602 ± 0.012	0.614 ± 0.012	$0.552^{+0.006}_{-0.005}$
σ^{fid}[nb]	4.68 ± 0.01 ± 0.14 ± 0.10	3.58 ± 0.01 ± 0.14 ± 0.08	0.781 ± 0.004 ± 0.008 ± 0.016
Acceptance A	0.383 ± 0.007	0.398 ± 0.007	0.393 ± 0.007
σ^{tot}[nb]	12.23 ± 0.03 ± 0.42 ± 0.27	9.00 ± 0.02 ± 0.39 ± 0.20	1.987 ± 0.011 ± 0.041 ± 0.042
	Muon channel (value ± stat ± syst ± lumi)		
Signal events	237720 ± 520 ± 2210 ± 410	183180 ± 460 ± 2520 ± 360	44706 ± 212 ± 9 ± 4
Correction C	0.653 ± 0.012	0.650 ± 0.012	0.711±0.008
σ^{fid}[nb]	4.50 ± 0.01 ± 0.09 ± 0.10	3.48 ± 0.01 ± 0.08 ± 0.08	0.777 ± 0.004 ± 0.008 ± 0.016
Acceptance A	0.383 ± 0.007	0.398 ± 0.007	0.393 ± 0.007
σ^{tot}[nb]	11.75 ± 0.03 ± 0.33 ± 0.27	8.75 ± 0.02 ± 0.25 ± 0.20	1.977 ± 0.009 ± 0.041 ± 0.042

W & Z masses in SM

$$m_W^2\left(1-\frac{m_W^2}{m_Z^2}\right)=\frac{\pi\alpha}{\sqrt{2}G_F}(1+\Delta r),$$

Where GF is the Fermi constant. Δr includes higher order corrections and is sensitive to top quark mass and, logarithmically, to the mass of the Higgs. In extended theories, Δr receives contributions from additional particles and interactions, and the comparison of the measured and predicted values of m_W constitutes a strong probe of the effects induced by physics beyond the SM.

The current Particle Data Group world average of mW = 8038515 MeV is dominated by the CDF and D0 measurements performed at √s = 1:96 TeV.

Given the precisely measured values of , G_F and m_Z , and taking recent top-quark and Higgs-boson mass measurements, the SM prediction of m_W is m_W = 803588 MeV and m_W = 803628 MeV (different calculations). The SM prediction uncertainty of 8 MeV represents therefore a target for the precision of future measurements of m_W.

Toni Baroncelli:

Global EW fits - 1

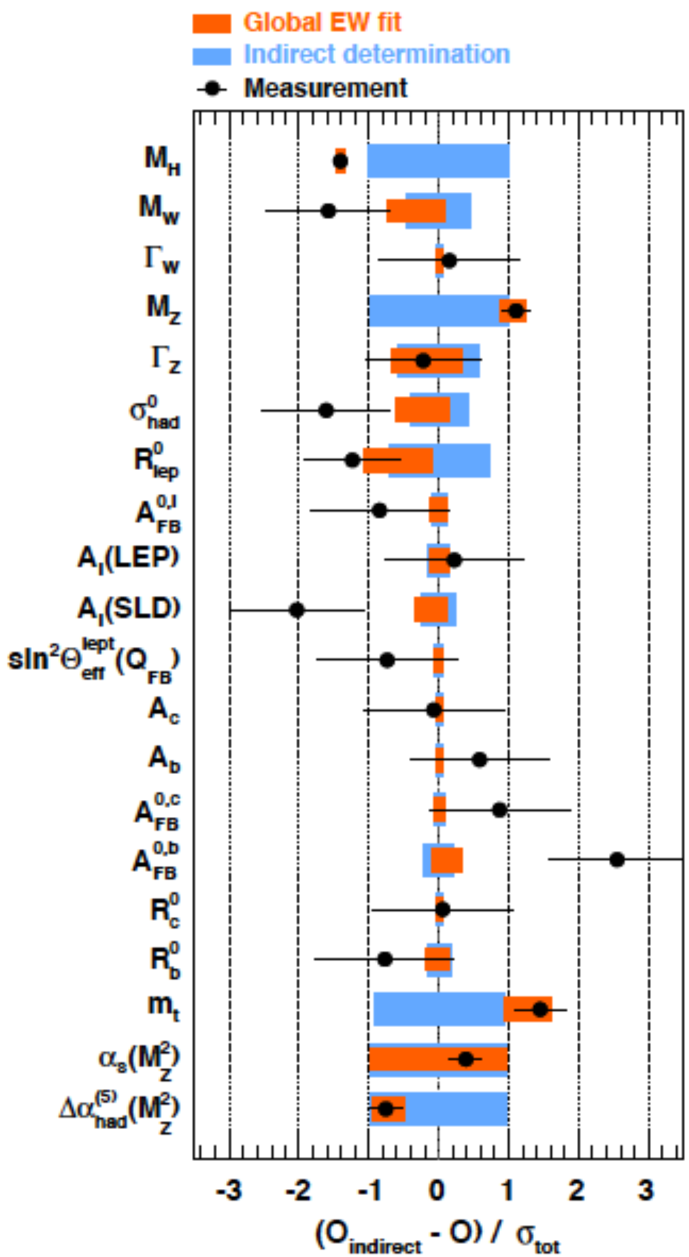

Comparison of the results with the indirect determination in units of the total uncertainty, defined as the uncertainty of the direct measurement and that of the indirect determination added in quadrature. The indirect determination of an observable corresponds to a fit without using the corresponding direct constraint from the measurement.

In the context of global fits to the SM parameters, constraints on physics beyond the SM are currently limited by the measurement of the W-boson mass. Therefore improving the precision of the measurements of m_W is of high importance for testing the overall consistency of the SM.

Global EW fits - 2

Parameter	Input value	Free in fit	Fit Result	w/o exp. input in line	w/o exp. input in line, no theo. unc
M_H [GeV]$^{(\circ)}$	125.14 ± 0.24	yes	125.14 ± 0.24	93^{+25}_{-21}	93^{+24}_{-20}
M_W [GeV]	80.385 ± 0.015	–	80.364 ± 0.007	80.358 ± 0.008	80.358 ± 0.006
Γ_W [GeV]	2.085 ± 0.042	–	2.091 ± 0.001	2.091 ± 0.001	2.091 ± 0.001
M_Z [GeV]	91.1875 ± 0.0021	yes	91.1880 ± 0.0021	91.200 ± 0.011	91.2000 ± 0.010
Γ_Z [GeV]	2.4952 ± 0.0023	–	2.4950 ± 0.0014	2.4946 ± 0.0016	2.4945 ± 0.0016
$\sigma^0_{\rm had}$ [nb]	41.540 ± 0.037	–	41.484 ± 0.015	41.475 ± 0.016	41.474 ± 0.015
R^0_ℓ	20.767 ± 0.025	–	20.743 ± 0.017	20.722 ± 0.026	20.721 ± 0.026
$A^{0,\ell}_{\rm FB}$	0.0171 ± 0.0010	–	0.01626 ± 0.0001	0.01625 ± 0.0001	0.01625 ± 0.0001
A_ℓ $^{(\star)}$	0.1499 ± 0.0018	–	0.1472 ± 0.0005	0.1472 ± 0.0005	0.1472 ± 0.0004
$\sin^2\theta^\ell_{\rm eff}(Q_{\rm FB})$	0.2324 ± 0.0012	–	0.23150 ± 0.00006	0.23149 ± 0.00007	0.23150 ± 0.00005
A_c	0.670 ± 0.027	–	0.6680 ± 0.00022	0.6680 ± 0.00022	0.6680 ± 0.00016
A_b	0.923 ± 0.020	–	0.93463 ± 0.00004	0.93463 ± 0.00004	0.93463 ± 0.00003
$A^{0,c}_{\rm FB}$	0.0707 ± 0.0035	–	0.0738 ± 0.0003	0.0738 ± 0.0003	0.0738 ± 0.0002
$A^{0,b}_{\rm FB}$	0.0992 ± 0.0016	–	0.1032 ± 0.0004	0.1034 ± 0.0004	0.1033 ± 0.0003
R^0_c	0.1721 ± 0.0030	–	$0.17226^{+0.00009}_{-0.00008}$	0.17226 ± 0.00008	0.17226 ± 0.00006
R^0_b	0.21629 ± 0.00066	–	0.21578 ± 0.00011	0.21577 ± 0.00011	0.21577 ± 0.00004
$\overline{m}_c$ [GeV]	$1.27^{+0.07}_{-0.11}$	yes	$1.27^{+0.07}_{-0.11}$	–	–
$\overline{m}_b$ [GeV]	$4.20^{+0.17}_{-0.07}$	yes	$4.20^{+0.17}_{-0.07}$	–	–
m_t [GeV]	173.34 ± 0.76	yes	$173.81 \pm 0.85^{(\bigtriangledown)}$	$177.0^{+2.3}_{-2.4}{}^{(\bigtriangledown)}$	177.0 ± 2.3
$\Delta\alpha^{(5)}_{\rm had}(M_Z^2)^{(\dagger\triangle)}$	2757 ± 10	yes	2756 ± 10	2723 ± 44	2722 ± 42
$\alpha_s(M_Z^2)$	–	yes	0.1196 ± 0.0030	0.1196 ± 0.0030	0.1196 ± 0.0028

$^{(\circ)}$Average of the ATLAS [48] and CMS [49] measurements assuming no correlation of the systematic uncertainties.
$^{(\star)}$Average of the LEP and SLD A_ℓ measurements [12], used as two measurements in the fit.
$^{(\bigtriangledown)}$The theoretical top mass uncertainty of 0.5 GeV is excluded.
$^{(\dagger)}$In units of 10^{-5}.
$^{(\triangle)}$Rescaled due to α_s dependence.

Table 2: Input values and fit results for the observables used in the global electroweak fit. The first and second columns list respectively the observables/parameters used in the fit, and their experimental values or phenomenological estimates (see text for references). The third column indicates whether a parameter is floating in the fit. The fourth column quotes the results of the fit including all experimental data. In the fifth column the fit results are given without using the corresponding experimental or phenomenological estimate in the given row (indirect determination). The last column shows for illustration the result using the same fit setup as in the fifth column, but ignoring all theoretical uncertainties. The nuisance parameters that are used to parameterise theoretical uncertainties are given in Table 1.

Strategy of the m_W measurement -1

- The mass of the W boson is extracted from the Jacobian edges of the final state kinematic distributions, measured in the plane perpendicular to the beam direction.
- Sensitive observables include the transverse momenta of the charged lepton and neutrino, and the W-boson transverse mass.
- ATLAS and CMS, benefit from large signal and calibration samples. The numbers of selected W- and Z-boson events, collected in a sample corresponding to approximately 4.6 fb^{-1} of integrated luminosity at a $\sqrt{s}$ = 7 TeV, are of the order of 10^7 for the W to lν and of the order of 10^6 for the Z to ll processes. The sizes of these samples correspond to a statistical uncertainty on m_W smaller than 10 MeV.
- ~25% of the W-production rate is induced by at least one s or c, in the initial state with implications on the W-boson transverse-momentum distribution. m_W is sensitive to the strange-quark and charm-quark parton distribution functions (PDFs) of the proton.

Strategy of the m_W measurement - 2

$$\vec{u}_T = \sum_i \vec{E}_{T,i}, \quad \vec{p}_T^{\,miss} = -\left(\vec{p}_T^{\,\ell} + \vec{u}_T\right). \quad m_T = \sqrt{2 p_T^{\ell} p_T^{miss}(1 - \cos\Delta\phi)},$$

- m_W is determined from fits to the transverse momentum of the charged lepton, p_l^T, and to the transverse mass of the W boson, m_T. For W bosons at rest, the transverse-momentum distributions of the W decay leptons have a Jacobian edge at a value of $m_W/2$, whereas the distribution of the transverse mass has an endpoint at the value of m, where m is the invariant mass of the charged-lepton and neutrino system, which is related to m_W through the Breit-Wigner distribution

$$\frac{d\sigma}{dm} \propto \frac{m^2}{(m^2 - m_V^2)^2 + m^4\Gamma_V^2/m_V^2}$$

- Templates are simulated for several values of m_W including signal and background contributions. The templates are compared to the observed distribution by means of a X^2 compatibility test. The measured values of m_W are determined by analytical minimisation of the X^2 function and interpolation between templates.

INFN ROMA Tre

Experimental aspects

- The Z to ll event samples are used to calibrate the detector response. Lepton momentum corrections are derived exploiting the precisely measured value of the Z-boson mass, m_Z , and the recoil response is calibrated using the expected momentum balance with p^T_{ll}. Identification and reconstruction efficiency corrections are determined from Z-boson events using the tag-and-probe method. The dependence of these corrections on p^T_l is important for the measurement of m_W, as it affects the shape of the template distributions.
- The detector response corrections and the physics modelling are verified in Z-boson events by performing measurements of the Z-boson mass with the same method used to determine the W-boson mass, and comparing the results to the LEP combined value of mZ , which is used as input for the lepton calibration.
- The determination of mZ from the lepton-pair invariant mass provides a first closure test of the lepton energy calibration.
- The p^{miss}_T and m_T variables are defined in Z-boson events treating one of the reconstructed decay leptons as a neutrino. The extraction of m_Z from the m_T distribution provides a test of the recoil calibration. The combination of the extraction of m_Z from the m_{ll}, p^l_T and m_T distributions provides a closure test of the measurement procedure. The accuracy of this validation procedure is limited by the size of the Z-boson sample, which is approximately ten times smaller than the W-boson sample.

Tuning the reconstruction

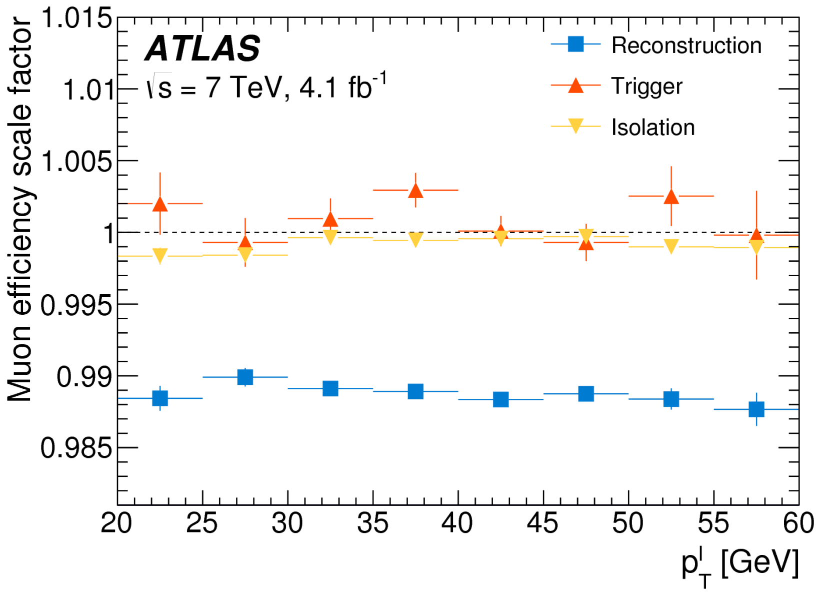

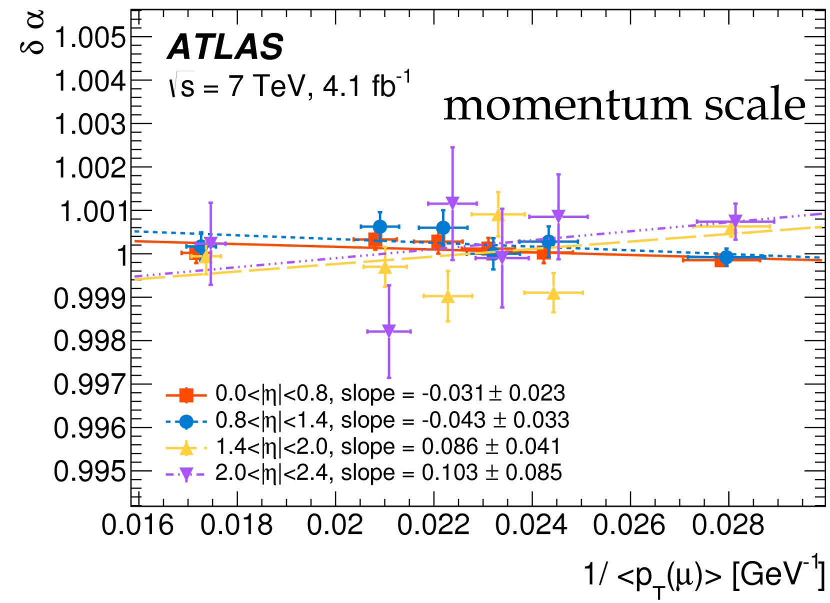

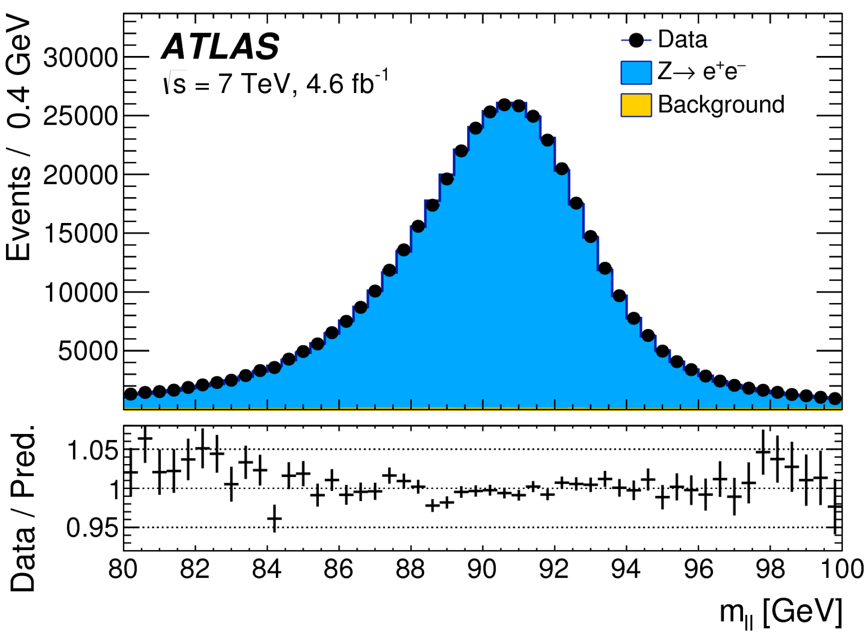

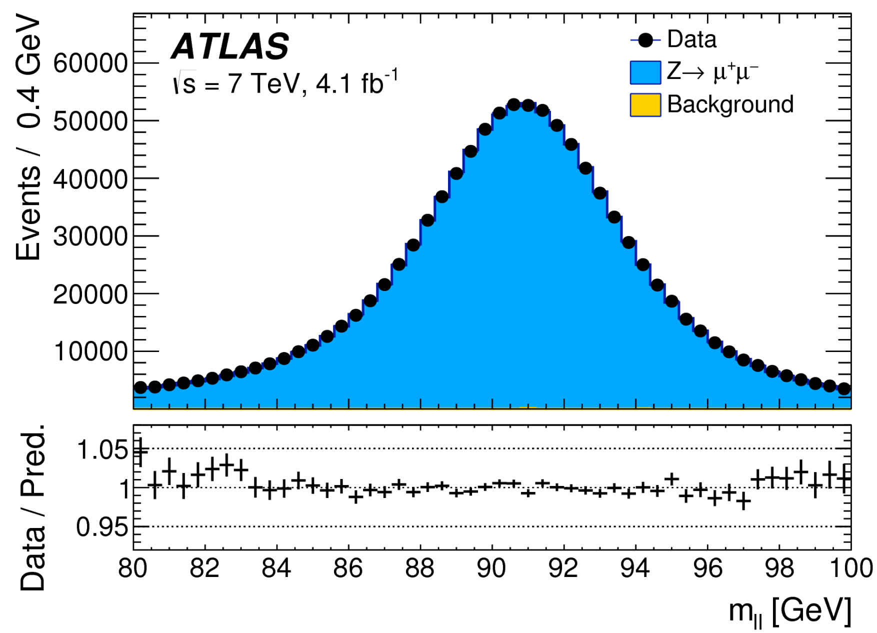

Toni Baroncelli:

mW measurement

Differential Z-boson cross section as a function of boson rapidity, and (b) differential W^+ and W^- cross sections as a function of charged decay-lepton pseudorapidity at $\sqrt{s}$=7 TeV. The measured cross sections are compared to the Powheg+Pythia 8 predictions, corrected to NNLO using DYNNLO with the CT10nnlo PDF set. The error bars show the total experimental uncertainties, including luminosity uncertainty, and the bands show the PDF uncertainties of the predictions.

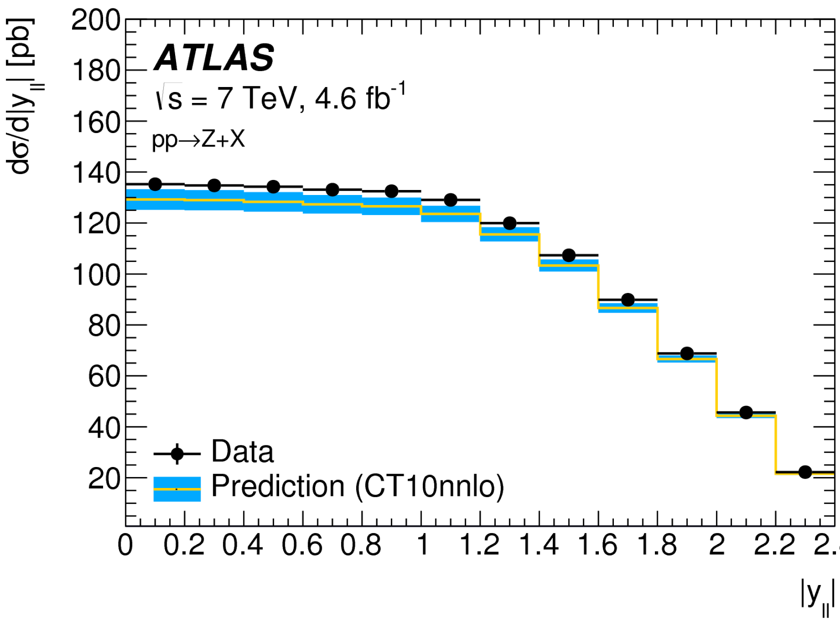

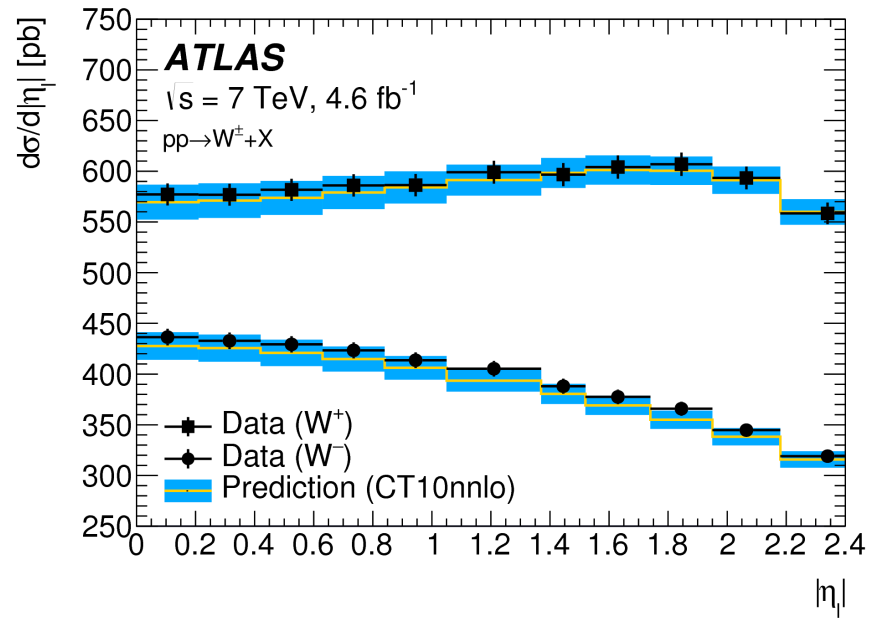

m_W : Results

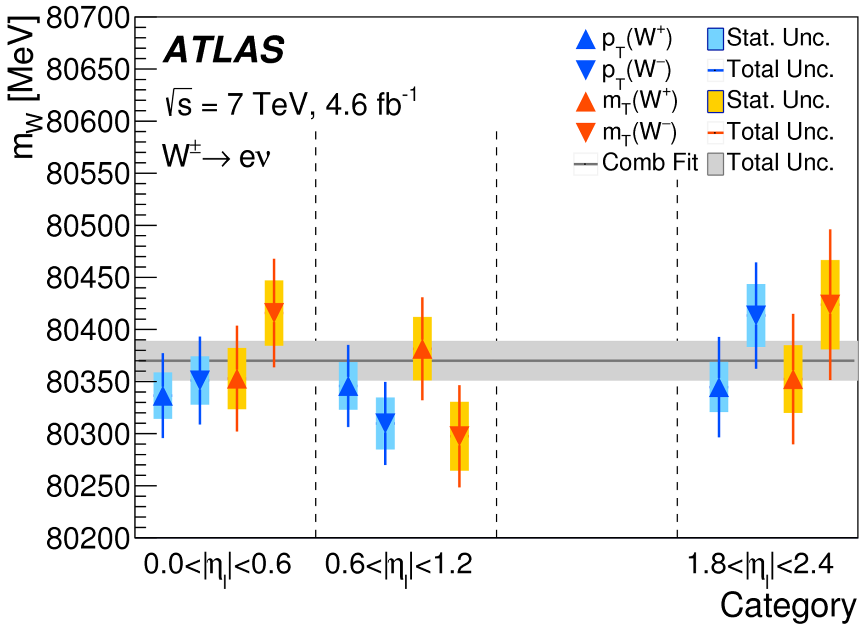

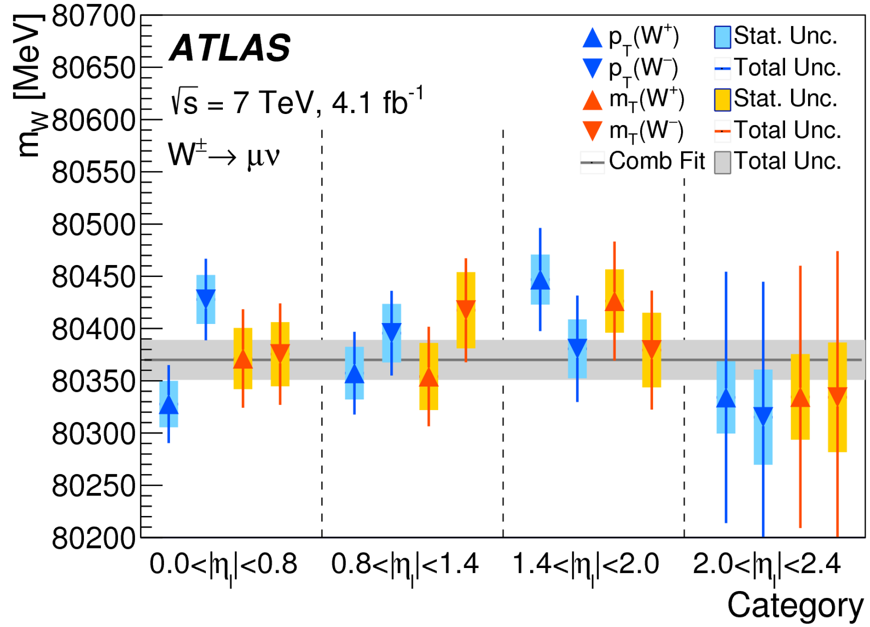

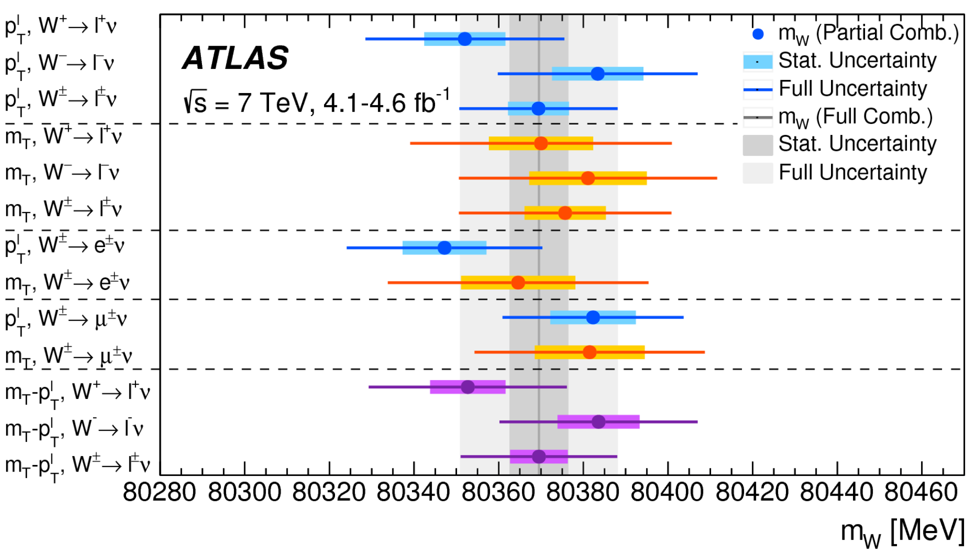

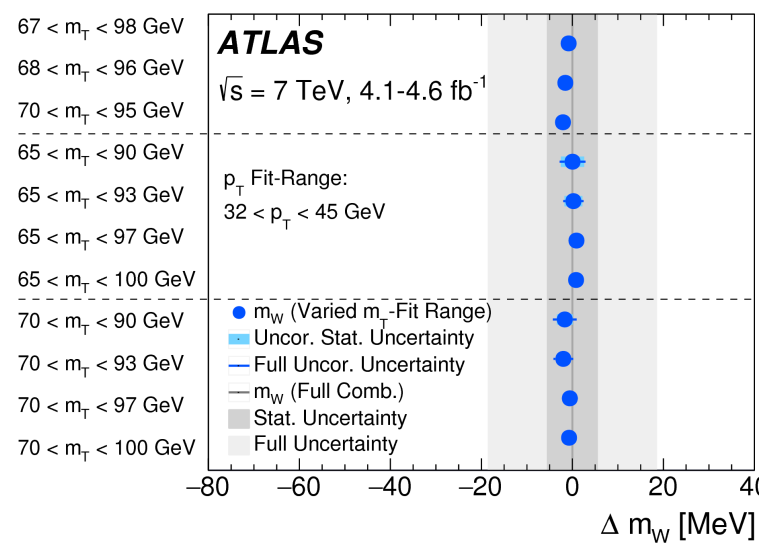

Toni Baroncelli:

Di-bosons

Toni Baroncelli:

Production mechanism

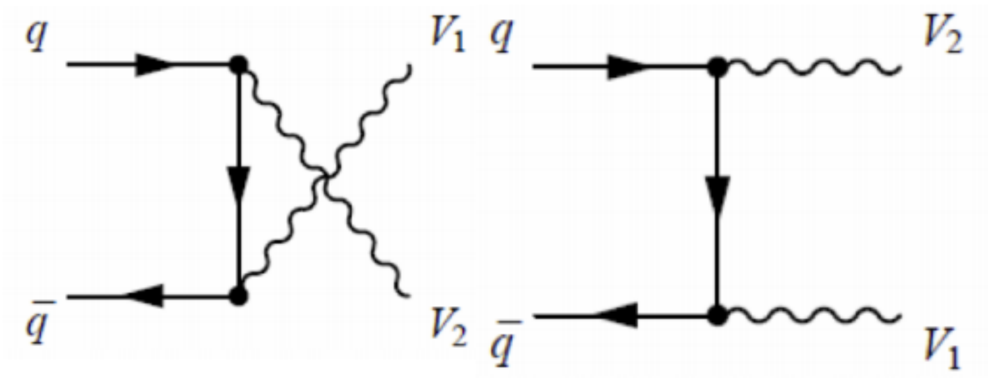

h to WW

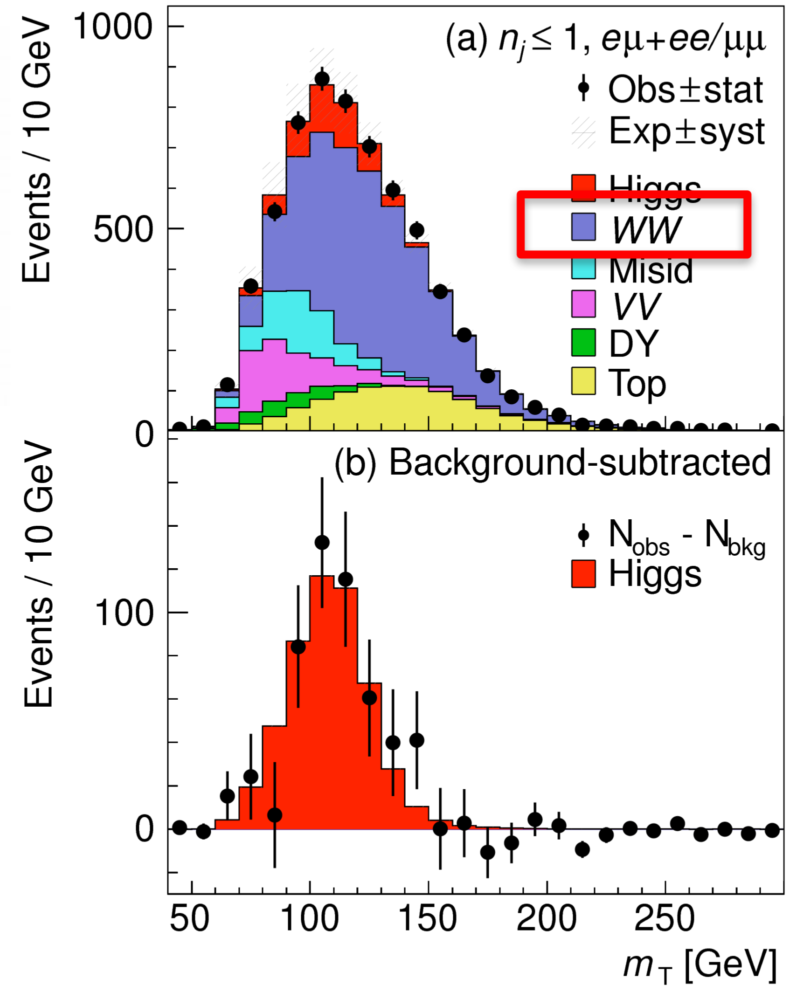

Why studying di-bosons?

- Stringent test of SM prediction in Electroweak sector and perturbative QCD at TeV scale
- background to many other channels, like Higgs Physics and exotic searches with leptons and large MET. In some cases may be irreducible

Di-bosons

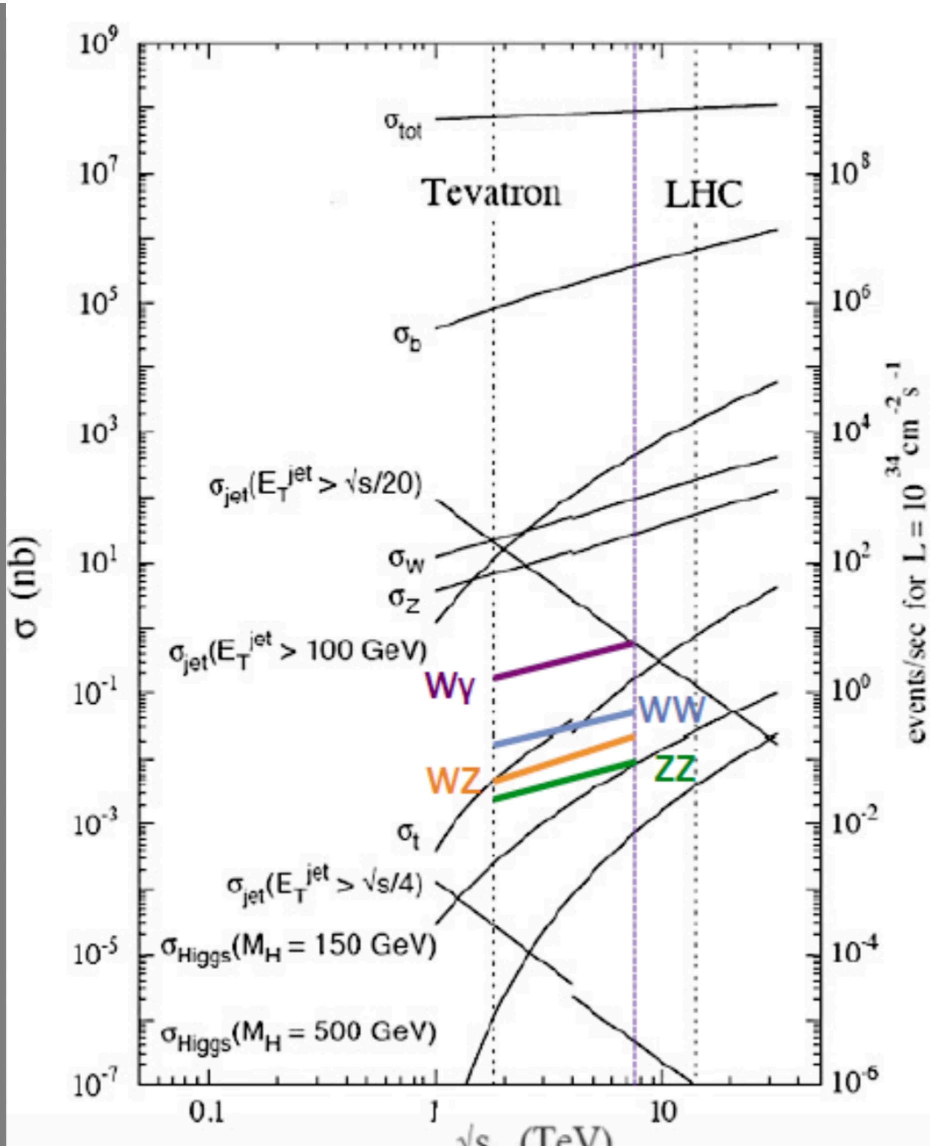

- Electroweak theory predicts triple and quartic gauge boson couplings (TGC, QGC).
- Due to new physics contribution TGC and QGC may deviate from SM prediction: anomalous couplings (neutral TGC's are forbidden at tree level).

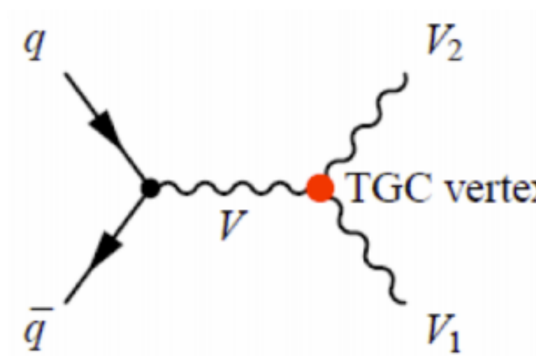

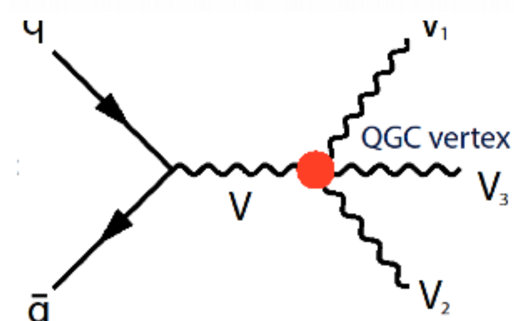

ATLAS compilation of di-bosons

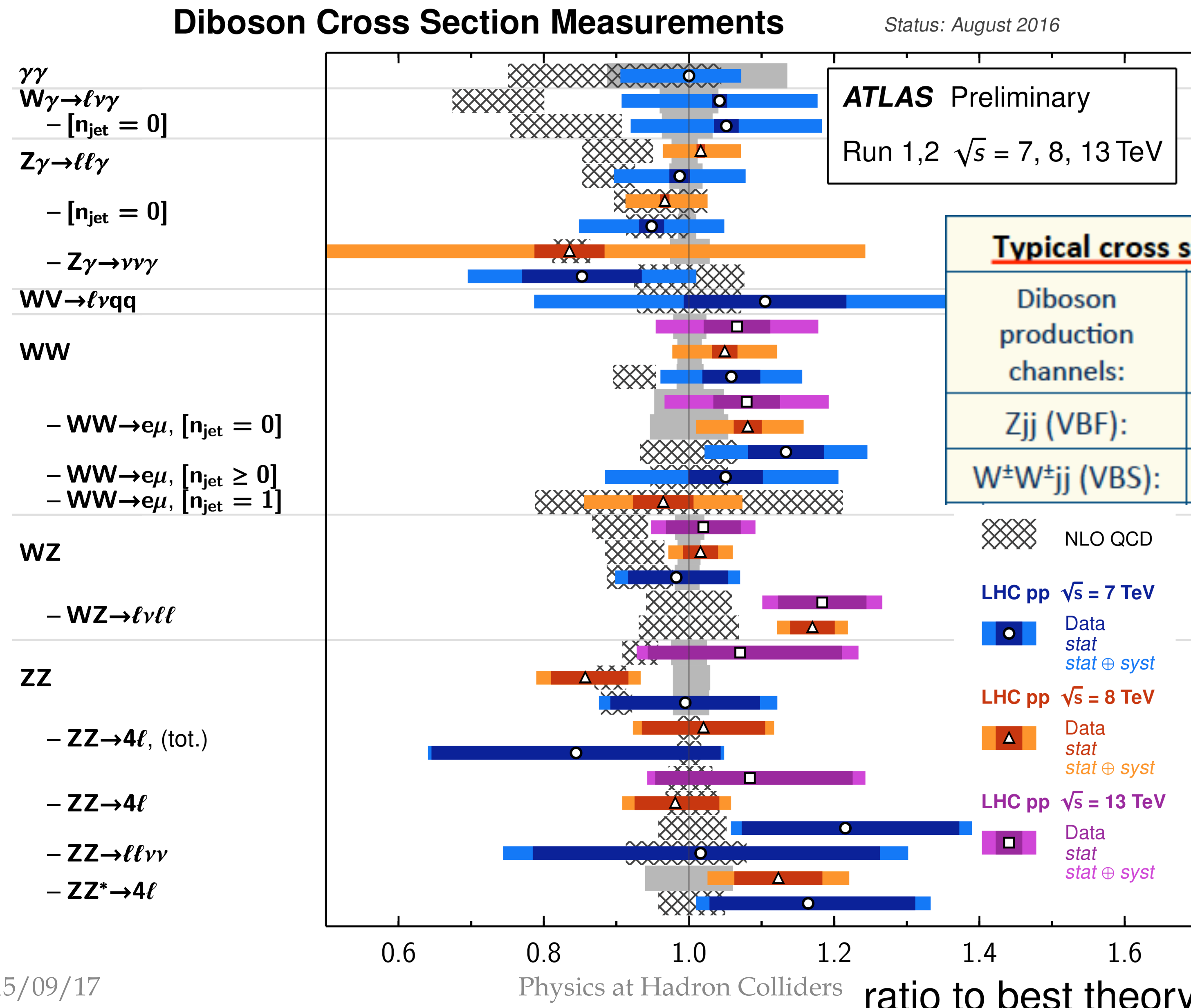

Typical cross section ranges	
Diboson production channels:	between 1 and 100 pb
Zjj (VBF):	about 50 fb
$W^{\pm}W^{\pm}jj$ (VBS):	some fb

PRL 116, 101801 (2016) PHYSICAL REVIEW LETTERS week ending 11 MARCH 2016

Measurement of the ZZ Production Cross Section in pp Collisions at $\sqrt{s} = 13$ TeV with the ATLAS Detector

G. Aad *et al.**
(ATLAS Collaboration)

(Received 17 December 2015; published 10 March 2016)

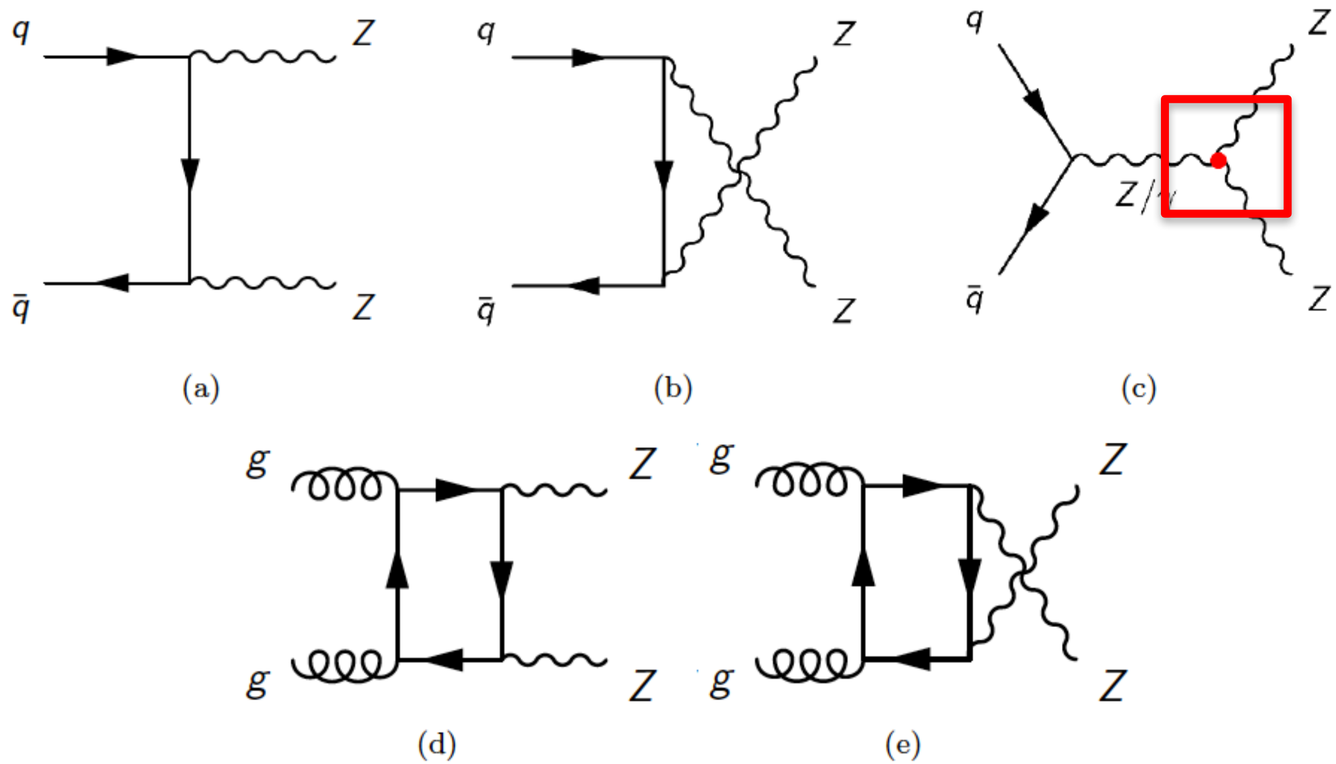

Figure 1. Leading order Feynman diagrams for ZZ production through the $q\bar{q}$ and gg initial state at hadron colliders. The s-channel diagram, (c), contains the $ZZ Z$ and $ZZ\gamma$ neutral TGC vertices which do not exist in the SM.

Selection of events

- Leptons: electrons & muons ; add γ to close *l* if $\sqrt{(\Delta\eta_{\ell,\gamma})^2 + (\Delta\phi_{\ell,\gamma})^2} < 0.1$
- Two pairs of leptons of same flavour and opposite charge; possible combinations : 2e2μ, 4e, 4μ. Mass of each pair between 66 and 116 GeV; in case of 4l of same flavour choose pairing which minimizes

$$|m_{ll,a} - m_Z| + |m_{ll,b} - m_Z|$$

- leptons well separated $\Delta R_{ll'} > 0.2$

A total of 63 events are observed in a sample of 3.2 0.2 fb^{-1} at $\sqrt{s}$ = 13 TeV, of which 15, 30, and 18 are in the 4e, 2e2μ, and 4μ channels, respectively.

MC simulation : scale factors are applied to the simulated events to correct for the small differences from data in the trigger, reconstruction, identification, isolation, and impact parameter efficiencies for electrons and muons . Furthermore, the lepton momentum scales and resolutions are adjusted to match the data.

Background estimation

Background originates from Z or W decaying to leptons + jets: heavy flavour decays, mis-identified jets, decays in flight. Compute this background using the data-driven estimation described below

- define "good lepton" a lepton which is isolated and with a small impact parameter
- define "jet-like-lepton" a lepton which fails only one of these criteria
- select a sample of events with 3 "good leptons" + 1 "jet-like-lepton"
- define

$$f = \frac{probability(non-1epton = full-lepton)}{probability(non-leptonlepton = jet-like-lepton)}$$

- the number of background events N(BG) is then

$$N(BG) = lllj * f + lljj * f^2$$

- Number of signal events has also to be increased by number of real ZZ events N(ZZ) where one lepton is identified as "jet-like-lepton" . This term is computed as $N(ZZ)_{MC} * f$
- f is measured using a sample of single-lepton triggered events with a Z boson candidate + a 3^{rd} lepton
    - f = # good-leptons / # jet-like-leptons

  after correcting, using MC, for real ZZ & ZW events

Toni Baroncelli:

ZZ to llll : Acceptance

N(BG) = 0.62 .1.08−0.11 events

A factor **C_{ZZ} is applied to correct for detector inefficiencies and resolution effects**. It relates the background subtracted number of selected events to the number in the fiducial phase space, and is defined as the ratio of generated signal events passing the selection criteria using reconstructed objects to the number passing the fiducial criteria using generator-level objects. C_{ZZ} is determined with a combination of the POWHEG ZZ MC sample and the SHERPA loop-induced gg-initiated sample. The C_{ZZ} value and its total uncertainty is determined to be 0.55 ± 0.02, 0.63 ± 0.02, 0.81 ± 0.03 in the 4e, 2e2μ, 4μ channel.

The cross section measured in the fiducial phase space is also extrapolated to the total phase space, which includes a correction for QED final-state radiation effects. The extrapolation factor is obtained from the same combination of MC samples as used in the C_{ZZ} determination. The ratio of the fiducial to full phase-space cross section is 0.39±0.02, in all three channels.

ZZ to llll : Results

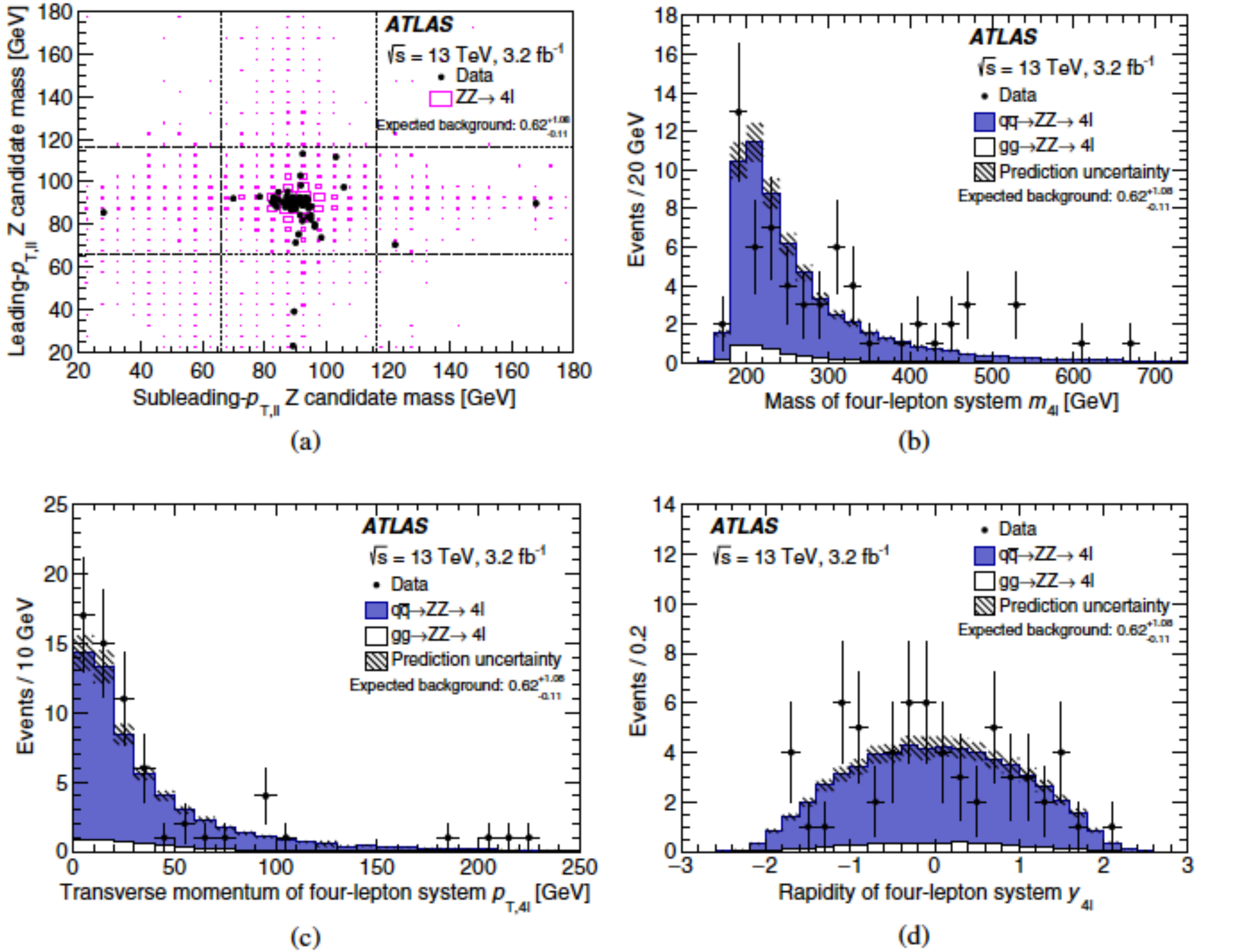

Results

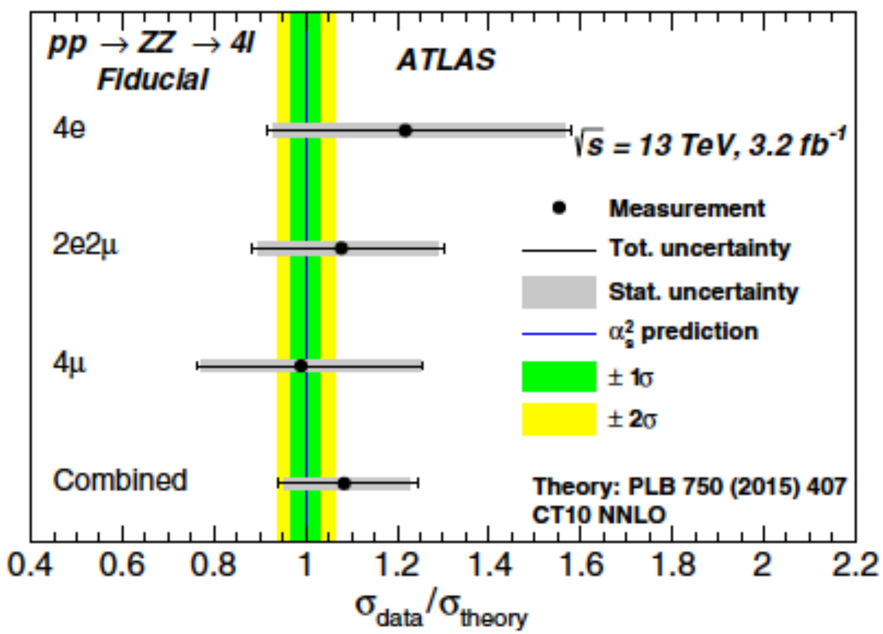

pp → ZZ → 4l
Fiducial
ATLAS
4e
2e2μ
4μ
Combined
√s = 13 TeV, 3.2 fb⁻¹
Measurement
Tot. uncertainty
Stat. uncertainty
α_s² prediction
± 1σ
± 2σ
Theory: PLB 750 (2015) 407
CT10 NNLO
0.4 0.6 0.8 1 1.2 1.4 1.6 1.8 2 2.2
σ_data/σ_theory

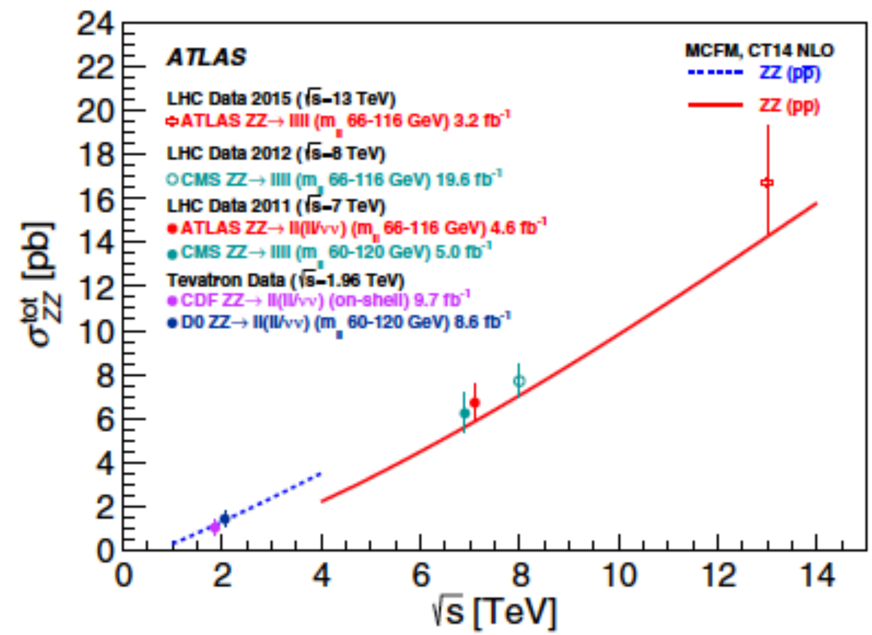

ATLAS
MCFM, CT14 NLO
ZZ (pp̄)
ZZ (pp)
LHC Data 2015 (√s=13 TeV)
ATLAS ZZ→ llll (m_ll 66-116 GeV) 3.2 fb⁻¹
LHC Data 2012 (√s=8 TeV)
CMS ZZ→ llll (m_ll 66-116 GeV) 19.6 fb⁻¹
LHC Data 2011 (√s=7 TeV)
ATLAS ZZ→ ll(ll/νν) (m_ll 66-116 GeV) 4.6 fb⁻¹
CMS ZZ→ llll (m_ll 60-120 GeV) 5.0 fb⁻¹
Tevatron Data (√s=1.96 TeV)
CDF ZZ→ ll(ll/νν) (on-shell) 9.7 fb⁻¹
D0 ZZ→ ll(ll/νν) (m_ll 60-120 GeV) 8.6 fb⁻¹
σ_ZZ^tot [pb]
√s [TeV]

ZZ to *llll* and *llνν* in Run I

Measurement of the ZZ production cross section in proton-proton collisions at √s = 8 TeV using the ZZ ➔ $l^+l^-l'^+l'^-$ and ZZ➔ $l^+l^-\nu\nu$ decay channels with the ATLAS detector

JHEP01(2017)099

Fiducial Phase Space					
Selection	$e^-e^+e^-e^+$	$\mu^-\mu^+\mu^-\mu^+$	$e^-e^+\mu^-\mu^+$	$e^-e^+\nu\bar{\nu}$	$\mu^-\mu^+\nu\bar{\nu}$
Lepton p_T	> 7 GeV			> 25 GeV	
Lepton $\|\eta\|$	$\|\eta\|_{e_1,e_2,e_3} < 2.5$ $\|\eta\|_{e_4} < 4.9$	$\|\eta\|_\mu < 2.7$	$\|\eta\|_{e_1} < 2.5$, $\|\eta\|_{e_2} < 4.9$ $\|\eta\|_\mu < 2.7$	$\|\eta\|_e < 2.5$	$\|\eta\|_\mu < 2.5$
$\Delta R(\ell,\ell')$	> 0.2			> 0.3	
$m_{\ell^-\ell^+}$	$66 < m_{\ell^-\ell^+} < 116$ GeV			$76 < m_{\ell^-\ell^+} < 106$ GeV	
Axial-E_T^{miss}	–			> 90 GeV	
p_T-balance	–			< 0.4	
Jet veto	–			$p_{T\,jet} > 25$ GeV, $\|\eta\|_{jet} < 4.5$, and $\Delta R(e,\text{jet}) > 0.3$	

$-E_T^{miss}\cdot\cos(\Delta\phi(\vec{E}_T^{miss},\vec{p}_T^{\,Z}))$

$|E_T^{miss} - p_T^Z|/p_T^Z$

Table 1. Fiducial phase-space definitions for each of the five ZZ final states under study.

$$\sigma^{fid}_{ZZ\to e^-e^+e^-e^+} = 6.2\,^{+0.6}_{-0.5}\ \text{fb}$$
$$\sigma^{fid}_{ZZ\to e^-e^+\mu^-\mu^+} = 10.8\,^{+1.1}_{-1.0}\ \text{fb}$$
$$\sigma^{fid}_{ZZ\to \mu^-\mu^+\mu^-\mu^+} = 4.9\,^{+0.5}_{-0.4}\ \text{fb}$$
$$\sigma^{fid}_{ZZ\to e^-e^+\nu\bar{\nu}} = 3.7 \pm 0.3\ \text{fb}$$
$$\sigma^{fid}_{ZZ\to \mu^-\mu^+\nu\bar{\nu}} = 3.5 \pm 0.3\ \text{fb}$$
$$\sigma^{total}_{pp\to ZZ} = 6.6\,^{+0.7}_{-0.6}\ \text{pb}$$

- 20.3 fb-1 , √s = 8 TeV
- single lepton triggers+isolation+p_T>24 GeV
- choice of primary vertex
- pairing in 4-electrons channel

Background calculation

Irreducible background

Source	$e^-e^+e^-e^+$	$\mu^-\mu^+\mu^-\mu^+$	$e^-e^+\mu^-\mu^+$	$\ell^-\ell^+\ell'^-\ell'^+$
ZZZ^*/ZWW^*	0.12 ± 0.01	0.19 ± 0.01	0.28 ± 0.02	0.58 ± 0.02
DPI	0.13 ± 0.01	0.15 ± 0.01	0.29 ± 0.01	0.57 ± 0.02
$t\bar{t}\,Z$	0.15 ± 0.03	0.16 ± 0.03	0.35 ± 0.05	0.66 ± 0.07
Total irreducible background	0.40 ± 0.04	0.50 ± 0.04	0.93 ± 0.05	1.82 ± 0.08

DPI = double proton interaction

Table 3. Number of events from the irreducible background SM sources that can produce four true leptons scaled to 20.3 fb^{-1}. The full event selection is applied along with all corrections and scale factors. The errors shown are statistical only.

"fake-leptons" background

Ingredients in eq. (7.1)	$e^-e^+e^-e^+$	$\mu^-\mu^+\mu^-\mu^+$	$e^-e^+\mu^-\mu^+$	Combined ($\ell^-\ell^+\ell'^-\ell'^+$)
$(+)N_{\text{data}}(\ell\ell\ell j) \times f$	8.6 ± 0.7	4.8 ± 2.4	16.0 ± 3.5	29.3 ± 4.3
$(-)N_{ZZ}(\ell\ell\ell j) \times f$	0.58 ± 0.01	1.96 ± 0.02	2.82 ± 0.02	5.36 ± 0.03
$(-)N_{\text{data}}(\ell\ell jj) \times f^2$	3.6 ± 0.1	1.0 ± 0.4	4.1 ± 0.6	8.8 ± 0.8
$(+)N_{ZZ}(\ell\ell jj) \times f^2$	0.00 ± 0.01	0.02 ± 0.08	0.02 ± 0.02	0.04 ± 0.02
Background estimate, N(BG)	4.4 ± 0.7 (stat) ± 2.8 (syst)	1.8 ± 2.4 (stat) ± 0.9 (syst)	9.0 ± 3.6 (stat) ± 3.9 (syst)	15.2 ± 4.4 (stat) ± 7.1 (syst)

Table 4. The number of ZZ background events from sources with fake leptons estimated using the data-driven fake-factor method in 20.3 fb^{-1} of data. The uncertainties quoted are statistical only, unless otherwise indicated, and combine the statistical uncertainty in the number of observed events of each type and the statistical uncertainty in the associated fake factor. The systematic uncertainty is shown for the background estimate in each final state.

Yelds

$ZZ \to \ell^-\ell^+\ell'^-\ell'^+$	$e^-e^+e^-e^+$	$\mu^-\mu^+\mu^-\mu^+$	$e^-e^+\mu^-\mu^+$	$\ell^-\ell^+\ell'^-\ell'^+$
Observed data	64	86	171	321
Expected signal	$62.2 \pm 0.3 \pm 2.6$	$83.7 \pm 0.4 \pm 3.2$	$141.6 \pm 0.6 \pm 4.0$	$287.0 \pm 0.8 \pm 8.1$
Expected background	$4.8 \pm 0.7 \pm 2.8$	$2.3 \pm 2.4 \pm 1.0$	$10.0 \pm 3.6 \pm 3.9$	$17.1 \pm 4.4 \pm 7.1$
$ZZ \to \ell^-\ell^+\nu\bar{\nu}$	$e^-e^+\nu\bar{\nu}$	$\mu^-\mu^+\nu\bar{\nu}$		$\ell^-\ell^+\nu\bar{\nu}$
Observed data	102	106		208
Expected signal	$51.1 \pm 0.9 \pm 2.6$	$55.1 \pm 1.0 \pm 2.9$		$106.2 \pm 1.3 \pm 3.9$
Expected background	$32.4 \pm 5.5 \pm 3.3$	$33.2 \pm 6.0 \pm 3.4$		$65.6 \pm 8.1 \pm 4.7$

Table 6. Summary of observed $ZZ \to \ell^-\ell^+\ell'^-\ell'^+$ and $ZZ \to \ell^-\ell^+\nu\bar{\nu}$ candidates in the data, total background estimates and expected signal for the individual decay modes and for their combination (last column). The first uncertainty quoted is statistical, while the second is systematic. The uncertainty in the integrated luminosity (1.9%) is not included.

Source	$e^-e^+\nu\bar{\nu}$	$\mu^-\mu^+\nu\bar{\nu}$
WZ	$16.7 \pm 1.1 \pm 1.7$	$18.5 \pm 1.0 \pm 1.5$
$ZZ \to \ell^-\ell^+\ell'^-\ell'^+$	$0.6 \pm 0.1 \pm 0.1$	$0.6 \pm 0.1 \pm 0.1$
$t\bar{t}$, W^-W^+, Wt, $ZZ \to \tau\tau\nu\nu$, $Z \to \tau^-\tau^+$	$13.3 \pm 3.2 \pm 0.2$	$15.4 \pm 3.6 \pm 0.3$
W + jets	$2.6 \pm 1.1 \pm 0.5$	$-0.9 \pm 0.7 \pm 1.0$
Z + jets	$-0.7 \pm 3.5 \pm 2.7$	$-0.5 \pm 3.8 \pm 2.9$
Total background	$32.4 \pm 5.5 \pm 3.3$	$33.2 \pm 6.0 \pm 3.4$

Control region eμ

Matrix method

Control region

Leptons not reconstructed, MC

Matrix Method

Definitions

- Prompt (P) and Fake (F) leptons TRUTH
- Signal (S) and Loose (L) regions RECONSTRUCTION
- Combinations N_{SS} .. N_{LL} … N_{PP}…N_{FF}

HP: the ratio the ratio of the number of signal leptons to the number of loose leptons is known separately for prompt and fake leptons

$$\begin{pmatrix} N_{SS} \\ N_{SL} \\ N_{LS} \\ N_{LL} \end{pmatrix} = \Lambda \cdot \begin{pmatrix} N_{PP} \\ N_{PF} \\ N_{FP} \\ N_{FF} \end{pmatrix}$$

$\text{lepton}_{1,2}$	signal/loose
fake	ε
prompt	ζ

$$\Lambda = \begin{pmatrix} \varepsilon_1\varepsilon_2 & \varepsilon_1\zeta_2 & \zeta_1\varepsilon_2 & \zeta_1\zeta_2 \\ \varepsilon_1(1-\varepsilon_2) & \varepsilon_1(1-\zeta_2) & \zeta_1(1-\varepsilon_2) & \zeta_1(1-\zeta_2) \\ (1-\varepsilon_1)\varepsilon_2 & (1-\varepsilon_1)\zeta_2 & (1-\zeta_1)\varepsilon_2 & (1-\zeta_1)\zeta_2 \\ (1-\varepsilon_1)(1-\varepsilon_2) & (1-\varepsilon_1)(1-\zeta_2) & (1-\zeta_1)(1-\varepsilon_2) & (1-\zeta_1)(1-\zeta_2) \end{pmatrix}$$

where ε_1 and ε_2 (ζ_1 and ζ_2) are the ratios of the number of signal and loose leptons for the leading and subleading prompt (fake) leptons, respectively.

Matrix method - 2

- prompt lepton efficiencies are determined from a data sample enriched with prompt leptons from $Z \longrightarrow l^+l^-$ decays, obtained by requiring $80 < m_{ll} < 100$ GeV;
- fake-lepton efficiencies are measured from a data set enriched with one prompt muon (by requiring it to pass the signal lepton selection and pT > 40 GeV) and an additional fake lepton (by requiring it to pass the loose selections)
- The fake-electron efficiency is determined from two samples of SS eμ events
- The fake-muon efficiency is determined from a sample of same-sign dimuon events

WZ production in Run II

Measurement of the $W^{\pm}Z$ boson pair-production cross section in pp collisions at $\sqrt{s}$ = 13 TeV with the ATLAS Detector

Phys. Lett. B 762 (2016) 1
DOI: 10.1016/j.physletb.2016.08.052

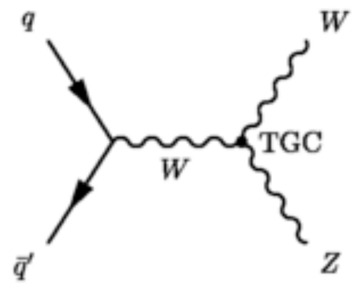

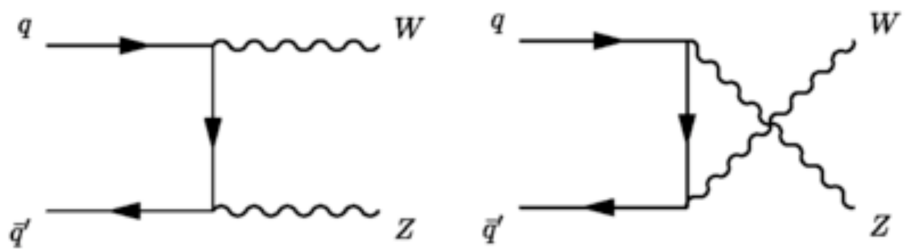

- Int. luminosity used = 3.2 fb^{-1}
- leptonic decays of Z & W (e+μ)
- $|\eta|$ leptons <2.5
- triggers, isolation, vertex
- exactly 3 leptons, pairing Z/W
- fiducial space defined by $p_T^l(Z) > 15$ GeV, $p_T^l(W) > 20$ GeV, $m_{ll}(Z)$ within 10 GeV from PDG value, $m_T^W > 30$ GeV, the angular distance ΔR between the charged leptons from the W and Z decay is larger than 0.3, and that ΔR between the two leptons from the Z decay is larger than 0.2

Extrapolate from fiducial volume to total cross section (take into account BR's)

yelds

reducible background (data-driven) & irreducible background (MC)

Channel	eee	μee	$e\mu\mu$	$\mu\mu\mu$	All
Data	98	122	166	183	569
Total expected	102 ± 10	118 ± 9	126 ± 11	160 ± 12	506 ± 38
WZ	74 ± 6	96 ± 8	97 ± 8	129 ± 10	396 ± 32
$Z + j, Z\gamma$	16 ± 7	7 ± 5	14 ± 7	9 ± 5	45 ± 17
ZZ	6.7 ± 0.7	8.7 ± 1.0	8.5 ± 0.9	11.7 ± 1.2	36 ± 4
$t\bar{t} + V$	2.7 ± 0.4	3.2 ± 0.4	2.9 ± 0.4	3.4 ± 0.5	12.1 ± 1.6
$t\bar{t}, Wt, WW + j$	1.2 ± 0.8	2.0 ± 0.9	2.4 ± 0.9	3.6 ± 1.5	9.2 ± 3.1
tZ	1.28 ± 0.20	1.65 ± 0.26	1.63 ± 0.26	2.12 ± 0.34	6.7 ± 1.1
VVV	0.24 ± 0.04	0.29 ± 0.05	0.27 ± 0.04	0.34 ± 0.05	1.14 ± 0.18

Table 1: Observed and expected numbers of events after the $W^{\pm}Z$ inclusive selection described in Section 5 in each of the considered channels and for the sum of all channels. The expected number of $W^{\pm}Z$ events from POWHEG+PYTHIA and the estimated number of background events from other processes are detailed. The total uncertainties quoted include the statistical uncertainties, the theoretical uncertainties in the cross sections, the experimental uncertainties and the uncertainty in the integrated luminosity.

Results

$$\sigma^{\text{fid.}}_{W^\pm Z\to\ell'\nu\ell\ell} = \frac{N_{\text{data}} - N_{\text{bkg}}}{\mathcal{L}\cdot C_{WZ}} \times \left(1 - \frac{N_\tau}{N_{\text{all}}}\right)$$

MC correction factor to account for τ decays to e,μ

C_{WZ} accounts for detector effects, resolution, efficiency (efficiency$_l^3$! $.9^3 = .7$)

Channel	C_{W^-Z}	C_{W^+Z}	$C_{W^\pm Z}$	N_τ/N_{all}
eee	0.428 ± 0.005	0.417 ± 0.004	0.421 ± 0.003	0.040 ± 0.001
μee	0.556 ± 0.006	0.550 ± 0.005	0.553 ± 0.004	0.038 ± 0.001
$e\mu\mu$	0.550 ± 0.006	0.553 ± 0.005	0.552 ± 0.004	0.036 ± 0.001
$\mu\mu\mu$	0.729 ± 0.007	0.734 ± 0.006	0.732 ± 0.005	0.040 ± 0.001

$$\sigma^{\text{tot.}}_{W^\pm Z} = \frac{\sigma^{\text{fid.}}_{W^\pm Z\to\ell'\nu\ell\ell}}{\mathcal{B}_W\,\mathcal{B}_Z\,A_{WZ}}$$

B_W, B_Z branching fractions, A_{WZ} is the MC computed acceptance

$$\sigma^{\text{fid.}}_{W^\pm Z\to\ell'\nu\ell\ell} = 63.2 \pm 3.2\,(\text{stat.}) \pm 2.6\,(\text{sys.}) \pm 1.5\,(\text{lumi.})\ \text{fb}.$$

$$\sigma^{\text{tot.}}_{W^\pm Z} = 50.6 \pm 2.6\,(\text{stat.}) \pm 2.0\,(\text{sys.}) \pm 0.9\,(\text{th.}) \pm 1.2\,(\text{lumi.})\ \text{pb}.$$